



# The CES EduPack DB for Bulk Functional Materials

Mike Ashby<sup>1</sup>, Tim Davies<sup>1</sup>, Stéphane Gorse<sup>2</sup>

Version 11, 2015  
© 2015 Granta Design Limited

## Abstract

The CES EduPack Functional Materials database is an extension of the existing Level 2 database to include records for piezoelectric, magnetic, magnetocaloric, magnetostrictive, semiconducting and thermoelectric materials. In total, records for 49 materials and 3 processes have been added, necessitating the creation of 40 new attributes. Notes linked to the attribute names in the records explain the underlying science. This White Paper describes the database, documents figures of merit (material indices) for material selection and gives examples of applications. Data are presented as 18 property charts made with the expanded database.



Device grade silicon boules and wafers. (Image courtesy of <http://www.chipsetc.com/silicon-wafers.html>)

## Table of Contents

|     |   |    |
|-----|---|----|
| 1.  | Introduction – What are Functional Materials? .....           | 2  |
| 2.  | Piezoelectric, Pyroelectric and Ferroelectric Materials ..... | 4  |
| 2.1 | Piezoelectric Materials .....                                 | 4  |
| 2.2 | Pyroelectric Materials .....                                  | 8  |
| 2.3 | Ferroelectric Materials .....                                 | 10 |
| 3.  | Magnetic Materials.....                                       | 15 |
| 3.1 | Ferromagnetic Materials .....                                 | 15 |
| 3.2 | Magnetostriction .....  | 21 |
| 3.3 | Magnetocaloric Materials.....                                 | 22 |
| 4.  | Semiconductors .....  | 26 |
| 4.1 | Semiconductors.....   | 26 |
| 4.2 | Thermoelectric Materials .....                                | 34 |
| 5.  | Case Studies .....  | 41 |
| 6.  | Conclusions .....   | 44 |
|     | Bibliography .....  | 44 |

<sup>1</sup> Engineering Department, Cambridge University and Granta Design, Cambridge, UK

<sup>2</sup> Bordeaux INP & Institut de Chimie de la Matière Condensée de Bordeaux, France.

# 1. Introduction – What are Functional Materials?

Although there is no standard definition of functional materials, it is commonly taken to mean materials with “interesting” properties that allow them to do more than simply support loads or conduct heat or electricity. Functional materials respond to applied stimuli in non-intuitive ways, for example generating a voltage upon application of strain or cooling on application of a magnetic field. Examples of this sort of property are listed in Table 1

| Input/Output          | Charge/Current                             | Magnetization        | Strain                        | Temperature                                | Light                   |
|-----------------------|--|----------------------|-------------------------------|--|-------------------------|
| <b>Electric Field</b> | <i>Permittivity</i><br><i>Conductivity</i> | Electro-magnetism    | Converse piezoelectric effect | Electrocaloric effect<br>Thermoelectricity | Electro-optic effect    |
| <b>Magnetic Field</b> | Magneto-electric effect                    | <i>Permeability</i>  | Magnetostriction              | Magnetocaloric effect                      | Magneto-optic effect    |
| <b>Stress</b>         | Piezoelectric effect                       | Piezomagnetic effect | <i>Elastic constant</i>       | -  | Photoelastic effect     |
| <b>Heat</b>           | Pyroelectricity<br>Thermoelectricity       | -                    | Thermal expansion             | <i>Specific heat</i>                       | -                       |
| <b>Light</b>          | Photovoltaic effect                        | -                    | Photostriction                | -  | <i>Refractive index</i> |

Table 1: A selection of stimuli and the possible responses to them. Standard responses are shown in italics; other properties are commonly viewed as functional properties (1).

Functional properties can be tuned by control of composition and dopants to meet particular design needs (Uchino, 2000) such as the harvesting of waste kinetic or thermal energy to provide locally-generated, clean, electrical power (Chung, 2010, Beeby et al, 2006) and digital and atomic scale actuation. Functional properties are found in every class of materials, including metals, polymers, ceramics and hybrids.

This White Paper describes an extension to the CES EduPack Level 2 database to include materials with interesting bulk (as opposed to surface) functional properties. Figure 1.1 lists the classes that appear in it. Figure 1.2 shows the record names and their location in the database structure.

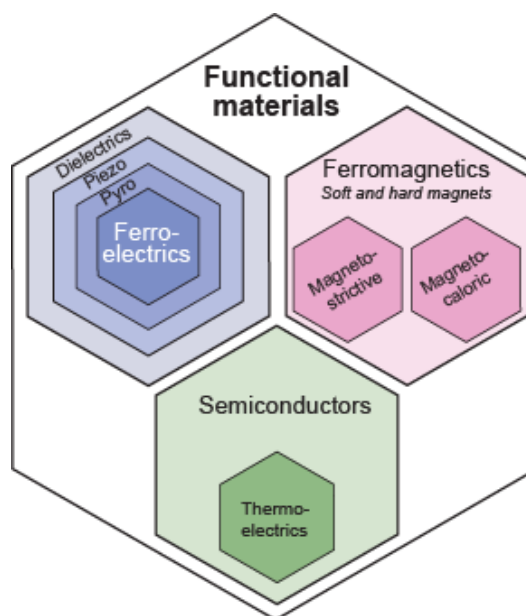


Figure 1.1 Classes of bulk functional materials



Figure 1.2. The tree structure of functional materials added to CES EduPack Level 2

## 2. Piezoelectric, Pyroelectric and Ferroelectric Materials

### Overview: Materials and Functional Attributes

| Record Name                              | Attribute                                   | Unit                              |
|--|---|-----------------------------------|
| Barium titanate                          | Piezoelectric charge coefficient, $d_{33}$  | pC/N                              |
| Bismuth titanate                         | Piezoelectric voltage coefficient, $g_{33}$ | mV.m/N                            |
| Lead lanthanum zirconium titanate (PLZT) | Electro-mechanical coupling constant, $k_p$ | -                                 |
| Lead zirconium titanate (PZT), hard      | Mechanical quality factor, $Q_m$            | -                                 |
| Lead zirconium titanate (PZT), soft      | Pyroelectric coefficient, $\gamma$          | $\mu\text{C}/\text{m}^2.\text{K}$ |
| Lithium niobate                          | Curie temperature (ferroelectric), $T_c$    | $^{\circ}\text{C}$                |
| Lithium tantalate                        | Spontaneous polarization                    | $\text{C}/\text{m}^2$             |
| Polyvinylidene fluoride (PVDF)           | Remanent polarization                       | $\text{C}/\text{m}^2$             |
| Quartz                                   | Coercive field                              | $\text{MV}/\text{m}$              |

### 2.1 Piezoelectric Materials

**Piezoelectric effect.** The piezoelectric effect appears in structures that lack a center of symmetry, so an atom at position (x, y, z) has no equivalent atom at point (-x, -y, -z). The distortion of a piezoelectric crystal by an applied stress causes positive and negative ions within the crystal to move relative to each other, changing the electronic dipole moment. On a macroscopic scale, this causes charge to appear at the faces of the crystal and a net potential difference to form across it.

**Piezoelectric charge coefficient,  $d_{33}$  (pC/N).** Consider a disc of piezoelectric material with electrodes covering the top and bottom surfaces. The application of a stress  $\sigma_{jk}$  creates a polarization  $P_i$  that is a linear function of the applied stress

$$P_i = d_{ijk} \sigma_{jk}$$

which gives with the use of the reduced-suffix notation:

$$P_i = d_{ij} \sigma_j \quad [\text{Eq. 1}]$$

where  $d_{ij}$  is the piezoelectric charge coefficient. If the loading is axial compression, the relevant coefficient is  $d_{33}$  relating polarization  $P_3$  to compressive stress  $\sigma_3$ .

**Piezoelectric voltage coefficient,  $g_{33}$  (mV.m/N).** The piezoelectric voltage coefficient,  $g_{33}$  relates electric field  $E$  to applied stress  $\sigma_{33}$

$$E_3 = g_{33} \sigma_3 \quad [\text{Eq. 2}]$$

Electric field is related to polarization by

$$E_3 = \frac{1}{\epsilon_r \epsilon_0} P_3 = \frac{d_{33}}{\epsilon_r \epsilon_0} \sigma_3,$$

meaning that  $g_{33} = \frac{d_{33}}{\epsilon_r \epsilon_0}$

where  $\epsilon_r$  is the relative permittivity (dielectric constant) and  $\epsilon_o$  the permittivity of vacuum ( $8.854 \times 10^{-12}$  F/m).

**Reverse piezoelectric effect,  $d_{33}$  (pC/N).** Applying an electric field to a piezoelectric material leads to relative motion of positive and negative atoms, resulting in a net shape change and strain. The strain generated by a field,  $E$ , is

$$\epsilon_i = d_{ij} E_j \quad [Eq. 3]$$

Conservation of energy requires that the same coefficient  $d_{ij}$  appears in both [Eq. 1] and [Eq.3].

**Electro-mechanical coupling constant,  $k_p$ .** When a field  $E$  is applied to a piezoelectric material, the electrical energy stored per unit volume is

$$W_{elec} = \frac{1}{2} \epsilon_r \epsilon_o E^2$$

The resulting piezoelectric strain stores elastic energy, which, per unit volume, is

$$W_{mech} = \frac{1}{2} \frac{\epsilon^2}{S}$$

where  $S$  is the elastic compliance and  $\epsilon$  is the strain.

The best single measure of the strength of the piezoelectric effect is the electro-mechanical coupling constant,  $k_p$ . It is defined in terms of its square,  $k_p^2$ , as

$$k_p^2 = (\text{mechanical energy converted to electrical energy}) / (\text{input mechanical energy})$$

or, equivalently (because the coupling is linear) as

$$k_p^2 = (\text{electrical energy converted to mechanical energy}) / (\text{input electrical energy})$$

Since the energy conversion is never 100% efficient,  $k_p < 1$ . Values of  $k_p$  range from 0.1 for quartz to 0.7 for PZT.

The ratio of the stored elastic energy to the input electrical energy.

$$k_p^2 = \left[ \frac{1}{2} \frac{(d_{33}E)^2}{S} \right] / \left[ \frac{1}{2} \epsilon_r \epsilon_o E^2 \right] = \frac{(d_{33})^2}{\epsilon_r \epsilon_o S} = \frac{d_{33} g_{33}}{S} \quad [Eq. 4]$$

**Mechanical quality factor.** The mechanical quality factor,  $Q_m$ , characterizes the sharpness of the electromechanical resonance spectrum. Its reciprocal,  $1/Q_m$ , is equal to the mechanical loss coefficient,  $\tan \delta_{mech}$ . The  $Q_m$  value is important in evaluating the magnitude and sharpness of the resonance peak. The vibration amplitude at an off-resonance frequency is amplified by a factor proportional to  $Q_m$  at the resonance frequency.  $Q_m$  is defined as:

$$Q_m = \frac{\omega_r}{2 \Delta\omega} = 2\pi \frac{\text{Energy stored}}{\text{Energy dissipated per cycle}} \quad [Eq. 5]$$

where  $\omega_r$  is the resonant frequency and  $2\Delta\omega$  is the width of the resonant peak at  $1/\sqrt{2}$  of the maximum height.

**Applications.** There are two major categories of piezoelectric devices: those that rely on the generator effect and those that rely on the motor effect.

**Generator effect.** The application of stress to a piezoelectric material leads to a potential difference, which can be large enough to generate a discharge - an effect used in gas lighters. The piezoelectric effect is used to measure very small displacements accurately by measuring the potential differences they generate. Vibrations of a body can be detected by a piezoelectric sensor in contact with it, an effect used in acoustic guitar pickups. Piezoelectric generators allow recovery of waste kinetic energy; piezoelectric floor tiles, for example, retrieve electrical power from the deflection cause by pedestrians (Yang and Caillat, 2006).

**Motor effect.** The converse piezoelectric effect – shape change due to the application of an electric field – enables atomic-scale actuation, used to control the sensing tip of atomic-force microscopes (AFMs). The same effect enables the quartz oscillator, the basis of most modern watches and other electronic devices that must keep accurate time. Piezoelectric devices can use both the generator and motor effects. An example is the ultrasonic probe in which a quartz resonator crystal acts both as generator and receiver of ultrasound waves.

**Performance metrics and charts for piezoelectric materials.**

Piezoelectric power generation is characterized by the material index  $d_{33} g_{33}$  (Eqn. 4). As Figure 2.1 shows, PZT has the highest value and for this reason it is used in energy-harvesting applications. PZT is a brittle material, a drawback for some devices. The piezoelectric polymer PVDF has a lower value of the index but it is flexible, an attractive feature when strains are large.

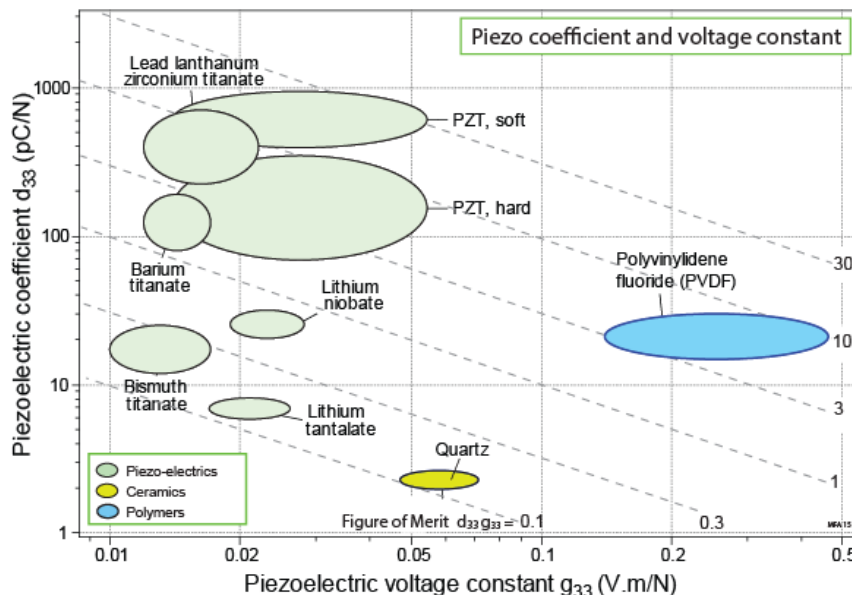


Figure 2.1. A chart of  $d_{33}$  against  $g_{33}$ . The common merit index  $d_{33}g_{33}$  is shown as dashed lines with a slope of -1

The performance index  $k_p^2 Q_m$  describes the energy absorption of piezoelectric materials at resonance (Colin et al, 2013). It is shown as diagonal contours on Figure 2.2, which also displays the two properties on which it depends. Among the materials plotted here quartz has by far the largest value of this index. It is for this reason that quartz is used so widely in

piezoelectric oscillators, where its extremely high mechanical quality factor allows stable oscillations at resonance.

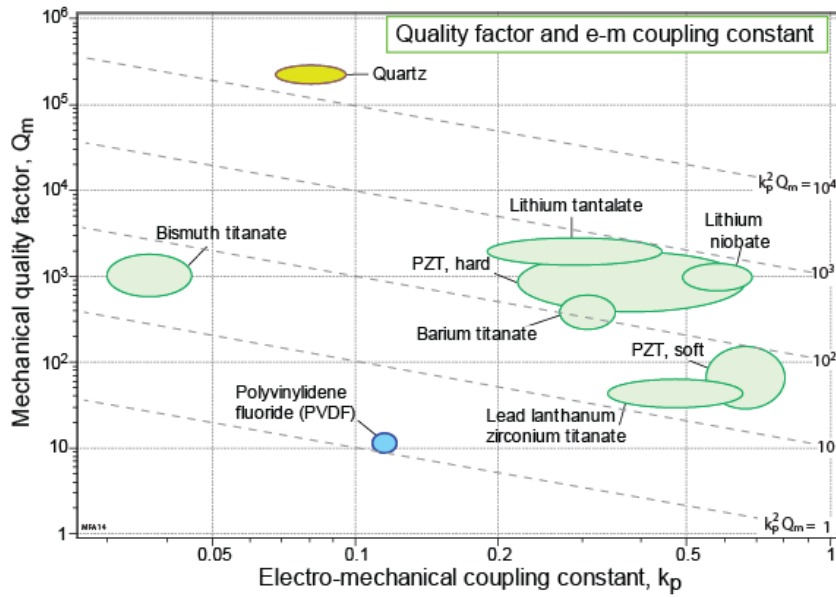


Figure 2.2. A plot of  $k_p$  against  $Q_m$ . The dashed lines represent materials with equal merit index  $k_p^2 Q_m$  and have a slope of 0.5

## 2.2 Pyroelectric Materials

**Pyroelectric effect.** Below the Curie temperature,  $T_c$ , crystals with a unique direction (a direction not repeated by any symmetry element) carry a permanent dipole (even in the absence of an applied field) because positive and negative charges do not cancel along the unique direction. When the temperature is constant the charged faces of the crystal attract opposite charges from the surroundings, screening the charge. But when the temperature changes, the positive and negative charges along the unique direction move relative to one another, changing the polarization as in Figure 2.3. This is known as the pyroelectric effect.

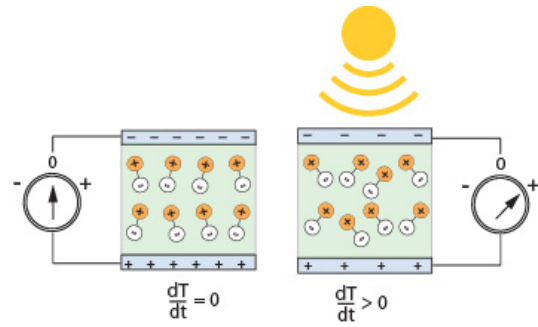


Figure 2.3: The pyroelectric effect

**Pyroelectric coefficient ( $\mu\text{C}/\text{m}^2\cdot\text{K}$ ).** The change in polarization  $\Delta P$  caused by a change of temperature  $\Delta T$  is given by

$$\Delta P = \gamma \Delta T$$

where  $\gamma$  is the pyroelectric coefficient. It depends on temperature, so the coefficient is best described by

$$\gamma(T) = \frac{\partial P}{\partial T}$$

Above the Curie temperature  $T_c$  the polarization is lost completely.

**Electrocaloric effect.** The electrocaloric effect is the change in temperature caused by a change of electric field. It arises because the field tends to align the dipoles, reducing the entropy, leading to a corresponding increase in temperature. Equivalently, removing the electric field allows disordering of the magnetic moments, increasing the entropy and causing a temperature decrease.

**Applications.** Pyroelectric materials are used in temperature sensors, infra-red detectors and thermal imaging. Examples are IR burglar alarms and thermal imaging for photography of wildlife at night – the heat radiated by the animal causes a change in the polarization at the detector or image-pixel. Pyroelectric materials have a fast response across a wide frequency spectrum and are effective at room temperature.

### Performance metrics and charts for pyroelectric materials.

Two material indices characterize pyroelectric materials. The first is the voltage responsivity,  $F_v$

$$F_v = \frac{\gamma}{\epsilon_r \rho C_p}$$

where  $C_p$  is the specific heat per unit mass,  $\rho$  is the density and  $\epsilon_r$  the dielectric constant. It is a measure of the potential difference generated by a given thermal input. It is shown in Figure 2.4 as diagonal contours. Lithium tantalate has the highest  $F_v$  among the materials

plotted here. It is commonly used in pyroelectric detectors (Beerman, 1975). In addition to a large pyroelectric coefficient, an ideal material for detector applications should have a small heat capacity in order to minimize the amount of heat required to raise its temperature, and a small dielectric constant to reduce the size of the detector, since these will result in large changes in voltage and temperature. Achieving large pyroelectric coefficient and small dielectric constant is difficult because these two parameters are not independently adjustable.

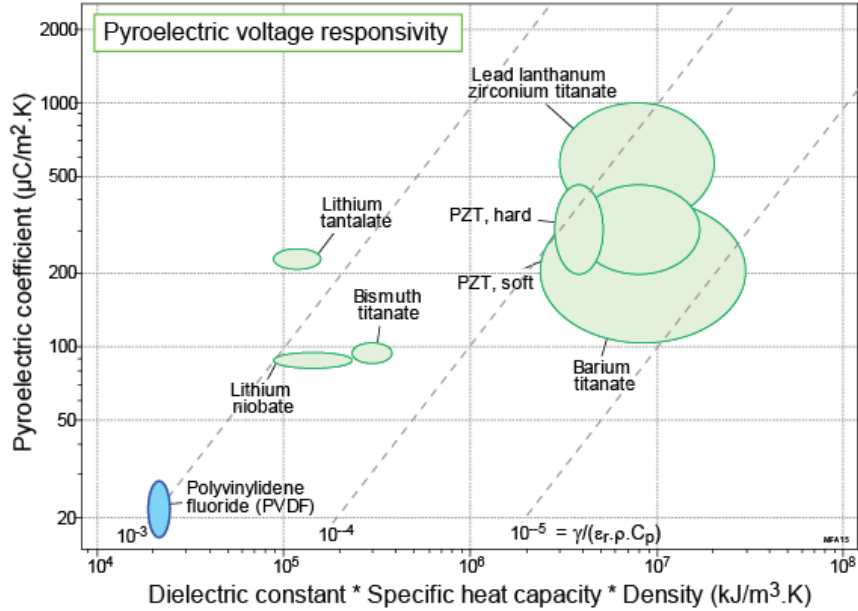


Figure 2.4. A plot showing the voltage responsiveness of pyroelectric materials. The dashed lines indicate materials of equal figure of merit

The second index for pyroelectric materials is the specific detectivity,  $F_D$ ,

$$F_D = \frac{\gamma}{\rho C_p (\epsilon_r \tan \delta)^{1/2}}$$

where  $\tan \delta$  is the dielectric loss tangent. This index, shown as diagonal contours in Figure 2.5, is important when noise from pyroelectric device makes up a considerable proportion of the signal. Again, lithium tantalate has the highest value.

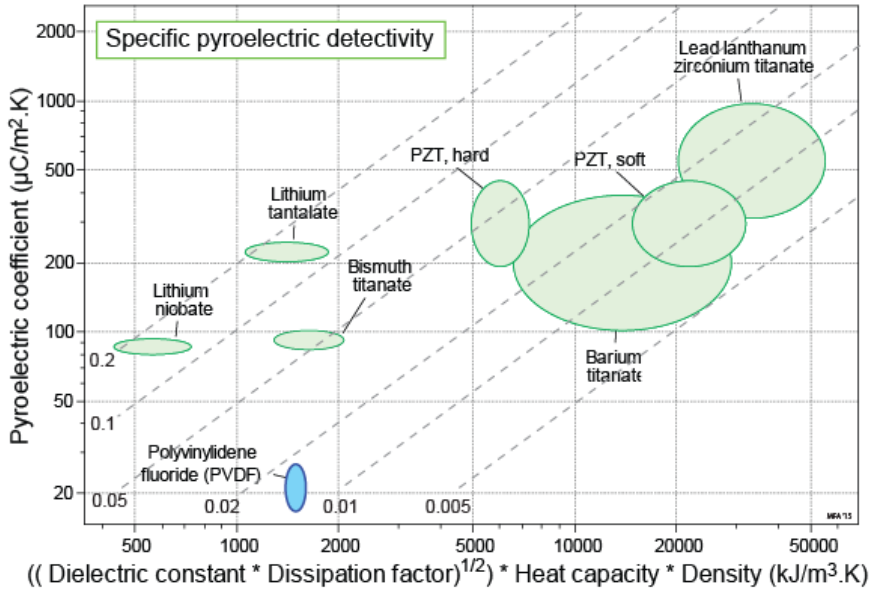


Figure 2.5. A plot of the specific detectivity of common pyroelectric materials. The dashed lines of gradient 1 represent equal values of  $F_D$

### 2.3 Ferroelectric Materials

**Curie temperature ( $^{\circ}\text{C}$ ) and Spontaneous polarization ( $\text{C}/\text{m}^2$ ).** Ferroelectric materials are a special case of pyroelectric behaviour, which in turn is a subclass of piezoelectric. Ferroelectrics, too, have an asymmetric structure, but have the ability to switch asymmetry. Barium titanate,  $\text{BaTiO}_3$ , shown schematically in Figure 2.6, is one of these. Below the Curie temperature (about  $120^{\circ}\text{C}$  for barium titanate) the titanium atom, instead of sitting at the center of the unit cell, is displaced up, down, to the left or to the right, as in (a) and (b), and ahead and behind in 3D. In ferroelectrics, these dipoles spontaneously align so that large volumes of the material are polarized even when there is no applied field. Above the Curie temperature the asymmetry disappears and with it the dipole moment, as at (c).

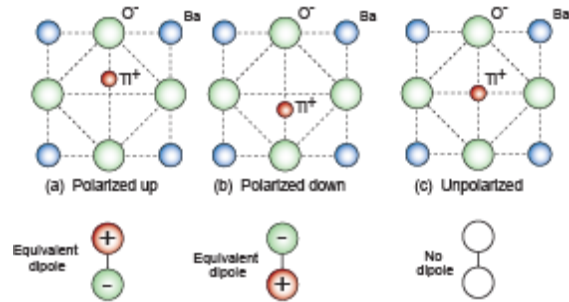


Figure 2.6: Barium titanate, below and above its Curie temperature

In the absence of an external field a ferroelectric divides itself up into *domains* – regions in which all the dipoles are aligned in one direction – separated by *domain walls* at which the direction of polarization changes as shown in Figure 2.7. The domains orient themselves so that the dipole moment of one more or less cancels those of its neighbors. If a field is applied the domain walls move so that the domains polarized parallel to the field grow and those polarized across or against it shrink, until the entire sample is polarized (or “poled”) in just one direction.

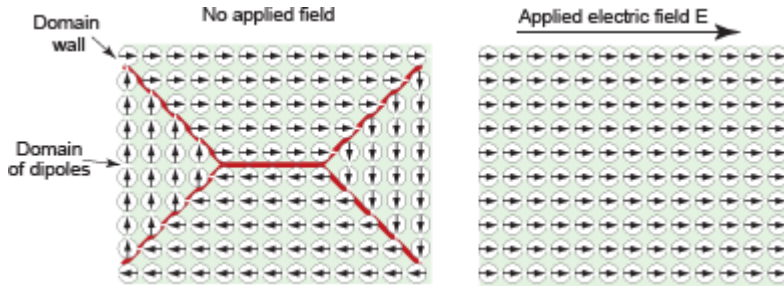


Figure 2.7: (a) Domains in a ferroelectric (b) After poling to align the dipoles

**Remanent polarization ( $C/m^2$ ) and coercive field (MV/m).** Ferroelectric materials exhibit a hysteresis curve (Figure 2.8). As the field  $E$  increases, the polarization  $P$  increases, reaching a maximum at the *saturation polarization*  $P_s$ . If the field is now removed, a large part of the polarization remains (the *remanent polarization*,  $P_r$ ), which is only removed by reversing the field to the value  $-E_c$ , the *coercive field*. The figure shows a complete cycle through full reverse polarization, ending up again with full forward poling. The little inserts show the domain structures around the cycle.

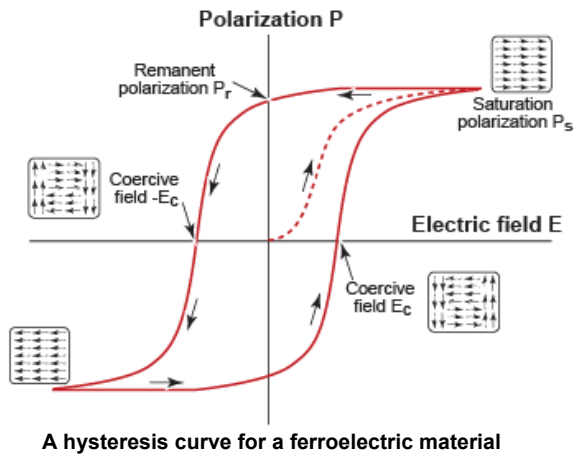


Figure 2.8 A hysteresis curve for a ferroelectric material

**Applications.** Ferroelectric materials are used mainly for their strong piezoelectric and pyroelectric properties or for their dielectric properties (Haertling, 1999). The dielectric constant  $\epsilon_r$  of materials with symmetric charge distributions lie in the range 2 to 20. Those for ferroelectrics can be as high as 20,000, allowing capacitors with a capacitance that can be 10,000 times greater than that of air based capacitors (Ertuğ, 2013). Such is the energy density that capacitors now compete with batteries for energy storage in kinetic energy recovery (KER) systems.

Ferroelectric materials allow electronic storage of data, although this is still less common than magnetic or optical storage media. In ferroelectric memory, an electric field is used to polarize a thin film of material, with the orientation of polarization representing the 0 and 1 binary states. This type of memory is found in RFID cards because it is cheap and compact.

**Performance metrics and charts for ferroelectric materials.** The amount of charge stored per unit voltage is called the capacitance,  $\chi$ :

$$\chi = \epsilon_r \epsilon_o \frac{A}{t}$$

where  $A$  is the area of the electrodes plates and  $t$  is the thickness of the dielectric. The energy density of a capacitor with a single dielectric layer increases with the square of the field  $E$ :

$$\text{Energy density} = \frac{1}{2} \epsilon_r \epsilon_o E^2$$

An upper limit for  $E$  is the dielectric strength,  $E_b$ , setting an upper limit for energy density:

$$\text{Maximum energy density} = \frac{1}{2} \epsilon_r \epsilon_o E_b^2$$

This upper limit is plotted as diagonal contours on Figure 2.9, which illustrates the enormous gains that ferroelectric ceramics offer. PZT has the highest value (and it is used for high performance capacitors) but barium titanate is the more usual selection because it is cheaper, easier to process, and lead-free.

Dielectric losses in barium titanate are reduced by doping. A typical barium titanate capacitor with  $E_b = 4 \text{ MV/m}$  and  $\epsilon_r = 2500$ , gives an energy density of  $177 \text{ kJ/m}^3$ . This is low compared with hydrocarbon fuels such as gasoline (energy density of about  $30,000 \text{ kJ/m}^3$ ) but is comparable with the batteries (nickel-cadmium battery has an energy density of approximately  $1000 \text{ kJ/m}^3$ ). However, it is worth noting that performance of various energy-storage devices is evaluated also by the power density, which is plotted against the energy density in Ragone chart of Figure 2.10. Supercapacitors have the highest power density which means they deliver energy more rapidly and can be charged more quickly than a battery.

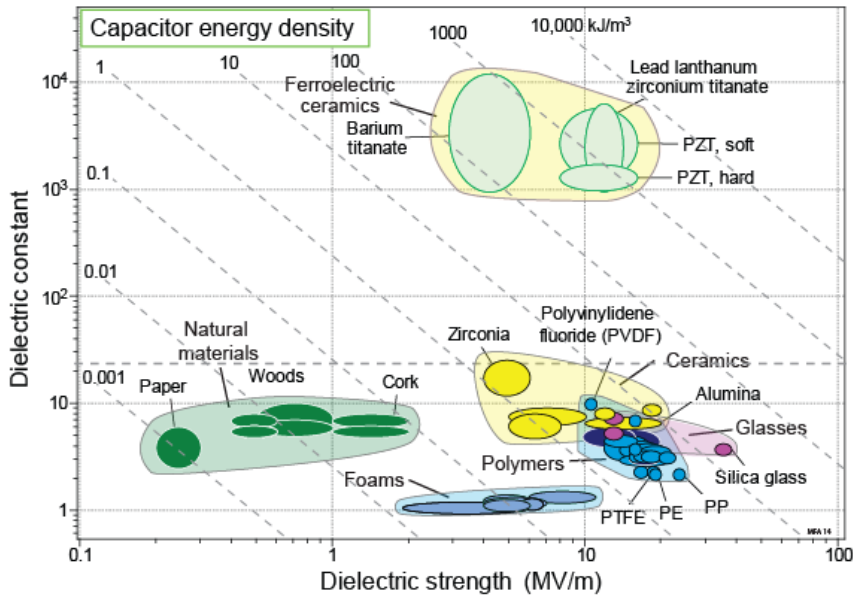


Figure 2.9. A plot showing the dielectric constant and strength of common materials. The ferroelectric ceramics have the highest energy density, represented by the dashed lines

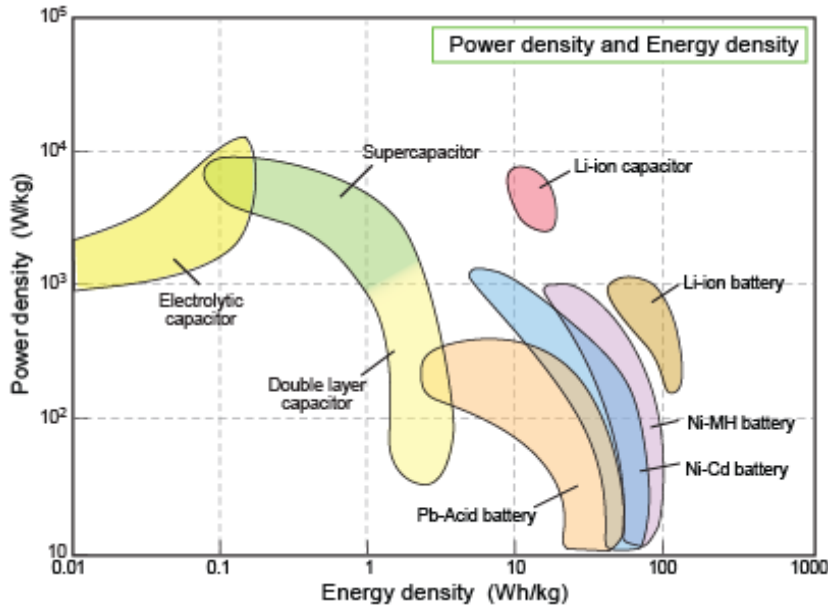


Figure 2.10. Power and energy density of energy storage systems

Materials for ferroelectric memory need a high remanent polarization and a low coercive field to allow polarized states to be switched with minimal energy loss – but not so low that they switch in the absence of an applied field. Figure 2.11 plots these two properties for common ferroelectric materials, illustrating why PZT is the most commonly used of these materials for ferroelectric memory.

The content of a typical record is shown below. Further information for Piezo, Pyro and Ferroelectric Materials can be found in Chung (2010), Haertling (1999), Holterman and Groen (2013), Jaffe (1971) and Uchino (2000).

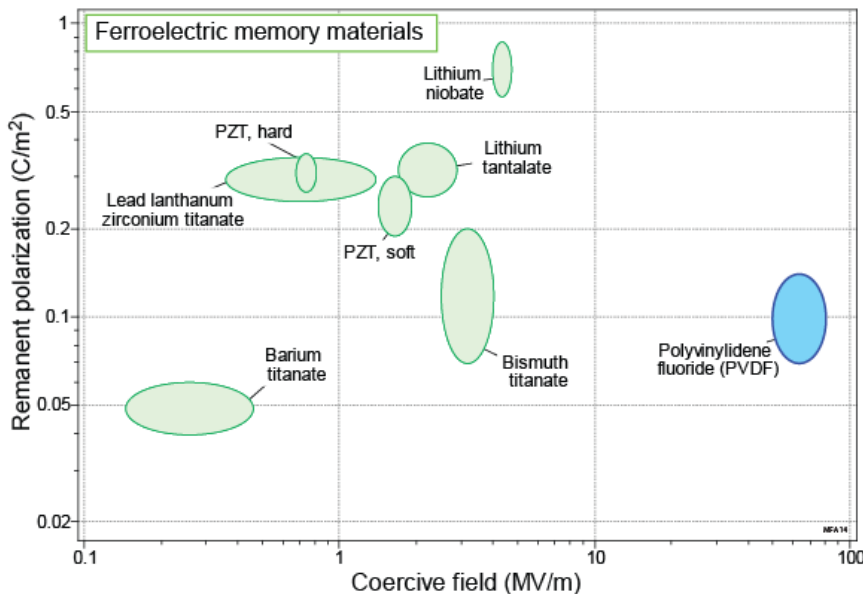


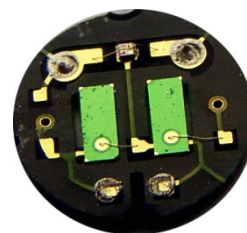
Figure 2.11. A plot of remanent polarization and coercive field for common ferroelectric materials. For ferroelectric memory, it is advantageous to have a low coercive field and a high remanent polarization. PZT is the commonly used material.

Typical record for a ferroelectric material

## Barium titanate

### The material

Barium titanate, BaTiO<sub>3</sub>, was the first polycrystalline ferroelectric ceramic to be discovered. It is commonly used in capacitors due to its extremely high dielectric constant. It was also used in piezoelectric devices, although PZT is now more common. In pure form it is an electrical insulator, but becomes semiconducting when doped with small amounts of metal (notably scandium, yttrium, neodymium or samarium). As a polycrystalline semiconductor it exhibits a positive temperature coefficient of resistivity, showing an increase in resistivity of several magnitudes at the Curie temperature, making it useful for thermistors and self-regulating heating systems.



Pyroelectric sensor (Image courtesy Nicolas Kruse).

### Typical uses

Capacitors; microphones and other transducers; thermistors; electro-optical modulation; capacitor energy storage for electric vehicles

### General properties

|                 |             |                   |
|-----------------|-------------|-------------------|
| Density         | 5500 - 6020 | kg/m <sup>3</sup> |
| Date first used | 1941        |                   |

### Thermal properties

|                          |           |            |
|--------------------------|-----------|------------|
| Melting point            | 1625      | °C         |
| Maximum service temp.    | 92 - 108  | °C         |
| Thermal conductivity     | 2.6 - 2.9 | W/m.°C     |
| Specific heat capacity   | 363 - 500 | J/kg.°C    |
| Thermal expansion coeff. | 6 - 11.4  | µstrain/°C |

### Mechanical properties

|                      |             |                      |
|----------------------|-------------|----------------------|
| Young's modulus      | 76          | GPa                  |
| Shear modulus        | 29.2 - 35.1 | GPa                  |
| Bulk modulus         | 55 - 65     | GPa                  |
| Poisson's ratio      | 0.27        |                      |
| Yield strength       | 59 - 100    | MPa                  |
| Tensile strength     | 59 - 100    | MPa                  |
| Compressive strength | 650 - 752   | MPa                  |
| Elongation           | 0.07 - 0.1  | % strain             |
| Hardness - Vickers   | 600 - 1100  | HV                   |
| Fracture toughness   | 0.65 - 1.8  | MPa.m <sup>0.5</sup> |

### Functional Properties

|               |      |
|---------------|------|
| Piezoelectric | True |
| Pyroelectric  | True |
| Ferroelectric | True |

### Piezoelectric properties

|                             |             |        |
|-----------------------------|-------------|--------|
| Piezoelectric voltage coef  | 12 - 17     | mV.m/N |
| Piezoelectric charge coef   | 82 - 190    | pC/N   |
| Electro-mechanical coupling | 0.27 - 0.35 |        |
| Mechanical quality factor   | 250 - 600   |        |

### Pyroelectric properties

|                          |           |                      |
|--------------------------|-----------|----------------------|
| Pyroelectric coefficient | 105 - 400 | µC/m <sup>2</sup> .K |
|--------------------------|-----------|----------------------|

### Ferroelectric properties

|                          |              |                  |
|--------------------------|--------------|------------------|
| Curie temperature        | 115 - 135    | °C               |
| Spontaneous polarization | 0.1 - 0.15   | C/m <sup>2</sup> |
| Remanent polarization    | 0.04 - 0.06  | C/m <sup>2</sup> |
| Coercive field           | 0.15 - 0.455 | MV/m             |

### Electrical properties

|                        |              |         |
|------------------------|--------------|---------|
| Electrical resistivity | 1e15 - 1e18  | µohm.cm |
| Dielectric constant    | 970 - 1.2e4  |         |
| Dissipation factor     | 0.003 - 0.03 |         |
| Dielectric strength    | 2.9 - 6      | MV/m    |

### Semiconductor properties

|          |     |    |
|----------|-----|----|
| Band-gap | 3.2 | eV |
|----------|-----|----|

### 3. Magnetic Materials

#### Overview. Materials and Functional Attributes

| Record Name                    |
|--------------------------------|
| Alnico                         |
| Amorphous iron alloys          |
| FeRh                           |
| Gadolinium                     |
| Galfenol                       |
| GdGeSi                         |
| Hard ferrites                  |
| La(Fe,Si)H                     |
| MnAs                           |
| MnFe(P,As)                     |
| MnNiGa                         |
| Neodymium iron boron           |
| Ni-Fe (45%)                    |
| Ni-Fe (75%)                    |
| Samarium cobalt                |
| Silicon iron transformer alloy |
| Soft ferrites                  |
| Terfenol-D                     |

| Attribute                           | Unit              |
|-------------------------------------|-------------------|
| Magnet type                         | Hard<br>Soft      |
| Curie temperature (magnetic)        | °C                |
| Remanent induction $B_r$            | T                 |
| Saturation induction $B_s$          | T                 |
| Coercive force $H_c$                | A/m               |
| Maximum energy product              | MJ/m <sup>3</sup> |
| Max permeability                    | No unit           |
| Saturation magnetostriction         | µstrain           |
| Adiabatic temperature change (0-2T) | °C                |
| Magnetic entropy change (0-2T)      | J/kg °C           |
| Operating temperature               | °C                |

#### 3.1 Ferromagnetic Materials

Nearly all materials respond to a magnetic field by becoming magnetized, but most are paramagnetic with a response so faint that it is of no practical use. *Ferromagnetic* and *ferrimagnetic* materials (*ferrites* for short), however, contain atoms that have large magnetic moments and with the ability to spontaneously magnetize – to align their moments in parallel – much as electric dipoles do in ferroelectric materials. These are of real practical use.

**Magnetic fields.** When a current  $i$  passes through a long, empty coil of  $n$  turns and length  $L$  as in Figure 3.1, a magnetic field is generated. The magnitude of the field,  $H$ , is given by Ampère's law as

$$H = \frac{ni}{L}$$

and thus has units of amps/meter (A/m).

The field induces a *magnetic induction* or *flux density*,  $B$ , which for vacuum or non-magnetic materials is

$$B = \mu_0 H$$

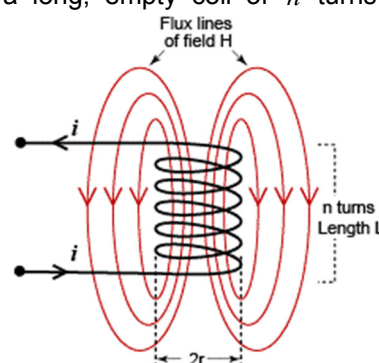


Figure 3.1: A solenoid creates a magnetic field  $H$ ; the flux lines indicate the field strength

where  $\mu_0$  is the permeability of vacuum,  $\mu_0 = 4\pi \times 10^{-7}$  henry/meter (H/m). The units of  $B$  are tesla, so a tesla is 1 HA/m<sup>2</sup>.

If the space inside the coil of is filled with a material, as in Figure 3.2, the induction within it changes. This is because its atoms respond to the field by forming little magnetic dipoles. The material acquires a macroscopic dipole moment or magnetization,  $M$  (its units are A/m, like  $H$ ). The induction becomes

$$B = \mu_0 (H + M)$$

The simplicity of this equation is misleading, since it suggests that  $M$  and  $H$  are independent; in reality  $M$  is the response of the material to  $H$ , so the two are coupled. If the material of the core is ferro-magnetic, the response is a very strong one and it is non-linear, as we shall see in a moment. It is usual to rewrite  $B$  in the form

$$B = \mu_R \mu_0 H$$

where  $\mu_R$  is the relative permeability. It is dimensionless. The magnetization,  $M$ , is thus

$$M = (\mu_R - 1)H = \chi H$$

where  $\chi$  is the magnetic susceptibility. Neither  $\mu_R$  nor  $\chi$  are constants – they depend not only on the material but also on the magnitude of the field,  $H$ , for the reason just given.

Magnetization decreases with increasing temperature. There is a temperature, the Curie temperature  $T_c$ , above which it disappears, as in Figure 3.3.

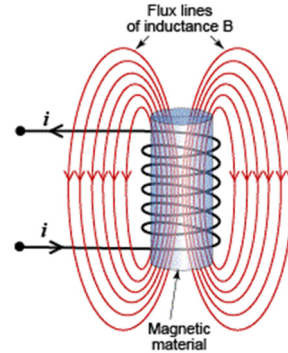


Figure 3.2: A magnetic material exposed to a field  $H$  becomes magnetized, concentrating the flux lines

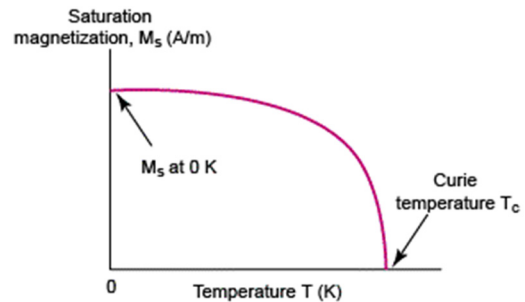


Figure 3.3: Saturation magnetization decreases with increasing temperature, falling to zero at Curie temperature  $T_c$ .

**Characterizing magnetic properties.** Magnetic properties are characterized by their  $M$ - $H$  or  $B$ - $H$  curve (the  $B$ - $H$  curve of a ferro-magnetic material looks very like its  $M$ - $H$  curve; it's just that the  $M$  axis has been scaled by  $\mu_0$ ). Figure 3.4 shows the  $M$ - $H$  for ferromagnetic material having magnetocrystalline anisotropy (in contrast to magnetically isotropic material that has no preferential direction for its magnetic moment, such as Gd). If an increasing field  $H$  is applied to a previously demagnetized sample, starting at point A on the figure, its magnetization increases, following the broken line, until it finally tails off to a maximum, the *saturation magnetization*  $M_s$  at the point B. If the field is now backed off,  $M$  does not retrace its original path, but retains some of its magnetization so that when  $H$  has reached zero, at the point C, some magnetization remains. it is called the *remanent magnetization* or *remanence*,  $M_R$ , and is usually only a little less than  $M_s$ . To decrease  $M$  further we must increase the field in the opposite direction until  $M$  finally passes through zero at the point D when the field is  $-H_c$ , the *coercive field*, a measure of the resistance to demagnetization. Some applications require  $H_c$  to be as high as possible, others, as low as possible. Beyond point D the magnetization  $M$  starts to increase in the opposite direction, eventually reaching saturation again at the point E. If the field is now decreased again  $M$  follows the  $M$ - $H$  curve through F and G back to full forward magnetic saturation again at B to form a closed circuit called the *hysteresis loop*.

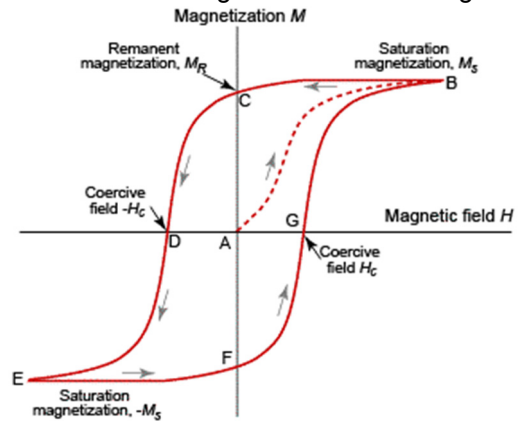


Figure 3.4: A hysteresis curve, showing the important magnetic properties

Magnetic materials differ greatly in the shape and area of their hysteresis loop, the greatest difference being that between *soft magnets*, which have thin loops, and *hard magnets*, which have fat ones, as sketched in Figure 3.5. In fact the differences are much greater than this figure suggests. the coercive field  $H_c$  (which determines the width of the loop) of hard magnetic materials like Alnico is greater by a factor of about  $10^5$  than that of soft magnetic materials like silicon-iron.

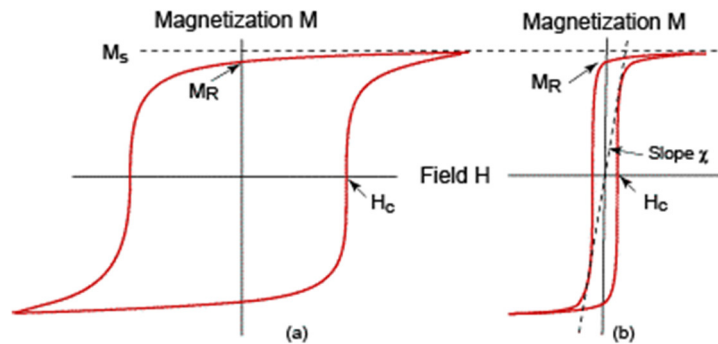


Figure 3.5: Hysteresis loops (a) a fat loop typical of hard magnets (b) a thin, square loop typical of soft magnets

**Performance metrics and charts for magnetic materials.** There are two major types of magnetic material; soft magnetic materials and hard magnetic materials (Figure 3.6). Soft magnetic materials have low coercive fields and narrow hysteresis loops. Hard magnetic materials have coercive fields that are many orders of magnitude higher.

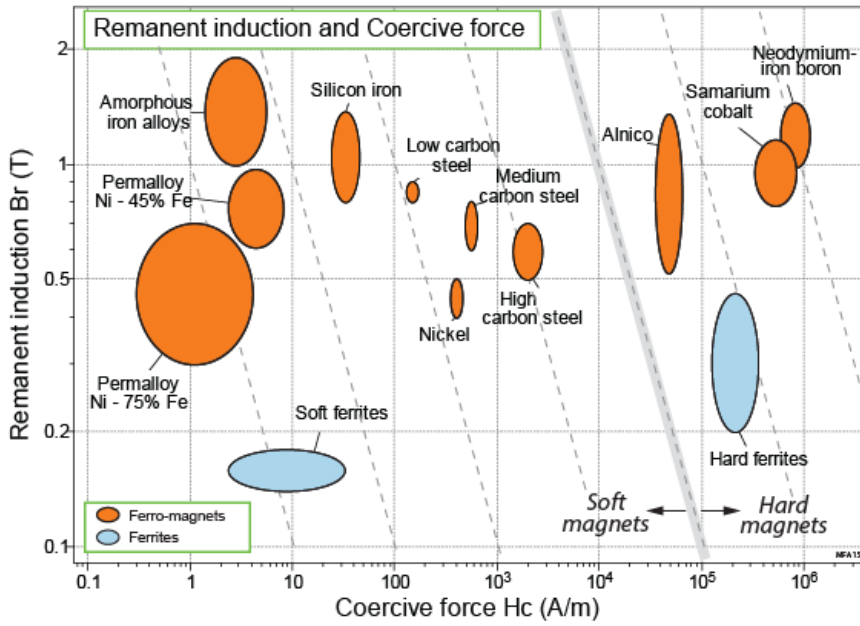


Figure 3.6. A plot of remanent induction and coercive force for common magnetic materials. There is a clear distinction between soft magnetic materials (to the left of the plot) and hard magnetic materials (to the right of the plot)

Soft magnetic materials are used for transformer cores and electromagnets, where they are used to trap and guide magnetic flux. Materials for these applications are chosen to have a large permeability, giving large inductance for a given applied magnetic field (Cardarelli, 2000). Eddy currents induced in the core by the magnetic field cause energy loss through resistive heating. Eddy currents, are reduced by high resistivity. Soft ferrites have the highest resistivity (Figure 3.7) and for that reason are used for radio frequency transformers, despite their relatively low permeability. The plot overstates the effect of eddy currents, which can be reduced by laminating layers of a silicon iron (for example) with an insulator to interrupt the conducting path. The Ni-Fe Permalloys have higher permeability than silicon iron but most transformers use silicon-iron because it is so much cheaper (Figure 3.7).

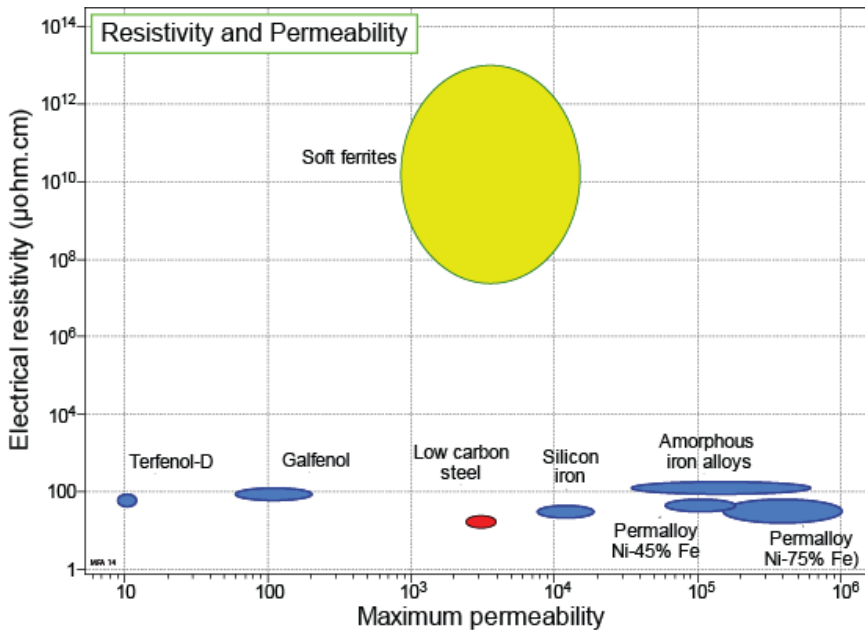


Figure 3.7. Permeability and resistivity of soft magnetic materials. As a ceramic, ferrites have a distinct advantage in terms of resistivity, but they have a low permeability and remanent induction.

Hard magnetic materials, used in permanent magnets, require high coercive fields (to prevent demagnetization) and high remanent inductions (to give a powerful, compact magnet). The figure-of-merit for permanent magnet materials is its *maximum energy product*, the maximum rectangular area that can be drawn under a hysteresis curve (Cardarelli, 2000). Neodymium-iron-boron magnets have the best permanent magnetic properties, with high coercive field and remanence (Figure 3.6). Samarium cobalt magnets have poorer magnetic properties than neodymium magnets but have higher operating temperatures and better corrosion resistance. When price is more important than magnetic performance, for example fridge magnets, hard magnetic ferrites are common. For magnets that must operate at high temperatures, alnicos are attractive (Figure 3.9) and they can also be cast into large and complex shapes.

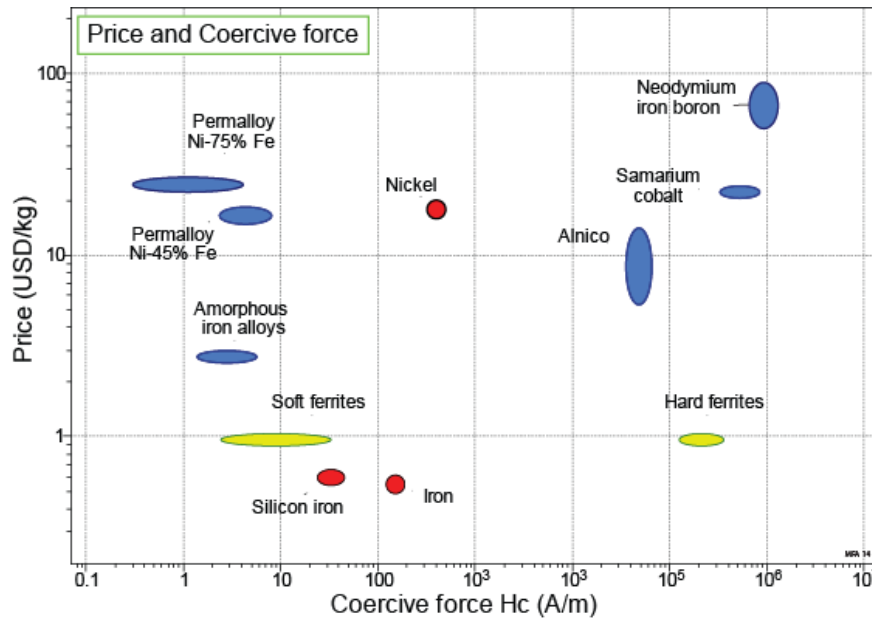


Figure 3.8 The price of common magnetic materials. Soft magnetic materials (with low coercive forces) are to the left of the plot, whilst hard magnetic materials are to the right.

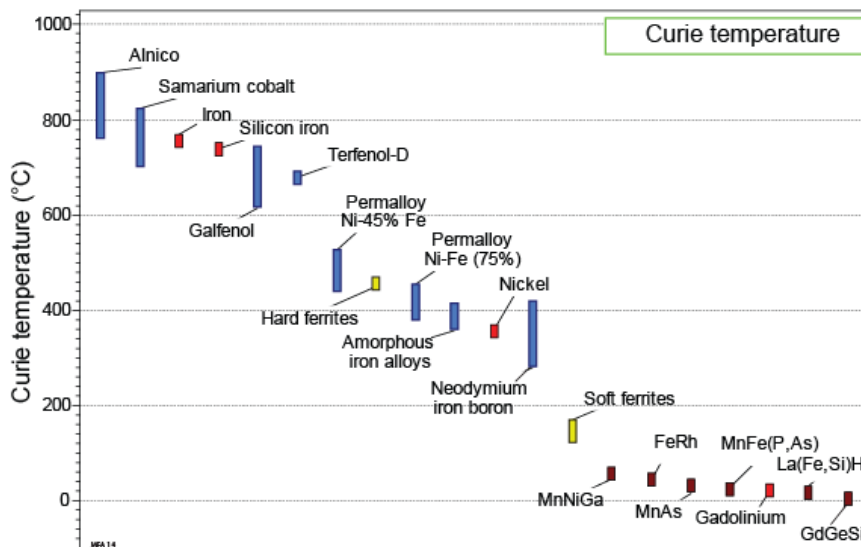


Figure 3.9. The Curie temperature of hard and soft magnets.

The content of a typical record is shown below.

Typical record for a ferromagnetic material

## Neodymium iron boron

### The material

Neodymium iron boron (NdFeB) is a very strong hard magnetic alloy, with the highest coercivity and energy product of any commercial magnetic alloy. This allows smaller magnets to be made than for other materials, and so they have replaced AlNiCo alloys in most applications where small magnets are required. NdFeB magnets are found in applications ranging from electric cars and wind turbines to hard disk drives and children's toys.



### Typical uses

Hard disk drives; headphone and speakers; electric motors; magnetic bearings; magnetic toys

### General properties

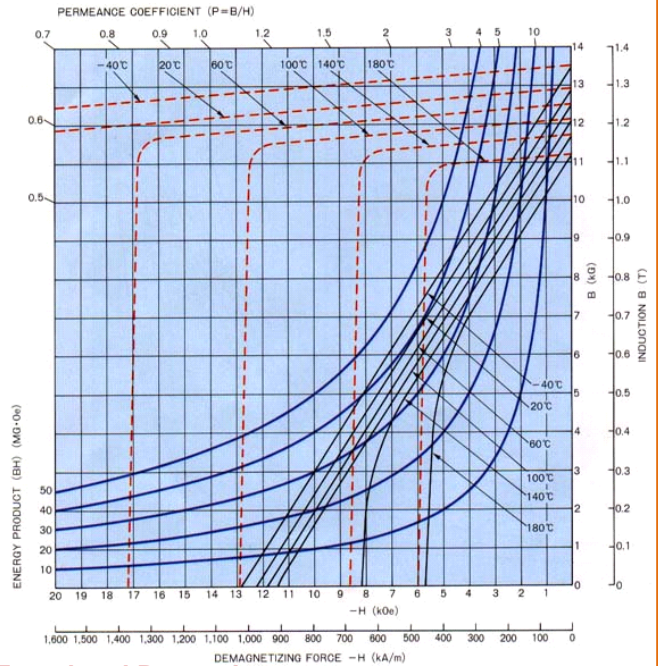
|         |             |                   |
|---------|-------------|-------------------|
| Density | 7400 - 7620 | kg/m <sup>3</sup> |
| Price   | 52.8 - 87.7 | USD/kg            |

### Thermal properties

|                          |             |            |
|--------------------------|-------------|------------|
| Melting point            | 1100 - 1300 | °C         |
| Maximum service temp.    | 80 - 210    | °C         |
| Thermal conductivity     | 8 - 10      | W/m.°C     |
| Thermal expansion coeff. | 3.4 - 4.8   | µstrain/°C |

### Mechanical properties

|                      |             |     |
|----------------------|-------------|-----|
| Young's modulus      | 152 - 157   | GPa |
| Shear modulus        | 43.3 - 71   | GPa |
| Bulk modulus         | 107 - 117   | GPa |
| Poisson's ratio      | 0.24        |     |
| Yield strength       | 78.4 - 82.7 | MPa |
| Tensile strength     | 78.4 - 82.7 | MPa |
| Compressive strength | 936 - 1130  | MPa |
| Hardness - Vickers   | 570 - 630   | HV  |



### Functional Properties

Ferromagnetic True

### Magnetic properties

|                              |                                   |
|------------------------------|-----------------------------------|
| Magnet type                  | Hard (Permanent magnet)           |
| Curie temperature (magnetic) | 280 - 420 °C                      |
| Remanent induction Br        | 0.98 - 1.45 T                     |
| Coercive force Hc            | 5.97e5 - 1.13e6 A/m               |
| Maximum energy product       | 1.91e5 - 3.82e5 MJ/m <sup>3</sup> |

### Electrical properties

|                        |            |
|------------------------|------------|
| Electrical resistivity | 150 µhm.cm |
|------------------------|------------|

### 3.2 Magnetostriction

**Magnetostriction** is shape change caused by a magnetic field. The field makes domain walls move, aligning the direction of magnetization and causing a strain. The material is described as having positive magnetostriction if its length increases with increasing magnetic field and negative magnetostriction if it does the opposite. The saturation magnetostriction is the maximum strain that can be induced in a material by applying a magnetic field sufficiently large to align the domains completely.

**Magneto-elastic effect.** When a solid is stressed, elastic energy is stored in it. If the solid is ferromagnetic and subject to a magnetic field, magnetic energy is also stored. The magneto-elastic effect describes the interaction of elastic and magnetic energies. The relation between these two energies is called magneto-mechanical coefficient of coupling  $k_{33}$ .

**Applications.** The electrical “hum” of transformers is due to magnetostriction of the transformer core, dissipating energy and reducing efficiency. For this reason transformer cores are made from materials with low magnetostriction such as the alloy 81.5wt%Ni–18.5wt%Fe. Nickel has negative magnetostriction and iron has positive; the composition is chosen such that the two effects cancel each other out.

The ability to convert magnetic energy into kinetic energy and vice-versa enables magnetic sensors and actuators, an effect exploited in sonar detection. For this application the best materials are so-called “giant magnetostrictive” materials – those with extremely high magnetostriction. Of these, Terfenol-D (an alloy of terbium, dysprosium and iron) is the most commonly used. An alternative is Galfenol (an alloy of gallium and iron) which is less brittle and requires a lower coercive field to saturate it.

**Performance metrics and charts for magnetostrictive materials.** Figure 3.10 is a chart of the saturation magnetostriction – the maximum strain made possible by a magnetic field.

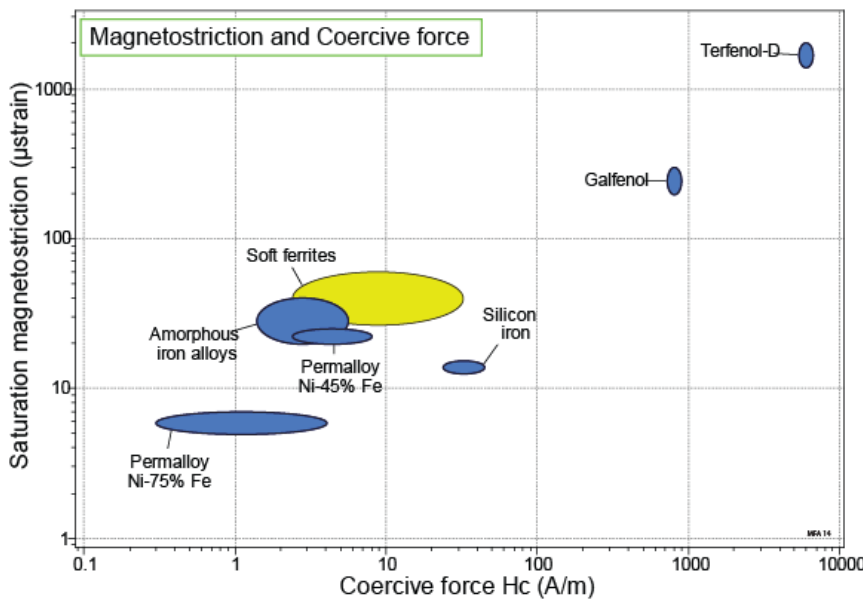


Figure 3.10 Saturation magnetostriction and coercive force for soft magnetic materials.

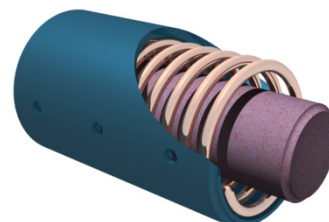
The content of a typical record is shown below. Further information for magnetostrictive materials can be found in Cardarelli (2000).

*Typical record for a magnetostrictive material*

## Terfenol-D

### The material

Terfenol-D, an alloy of terbium, dysprosium and iron (Tb<sub>0.3</sub>Dy<sub>0.7</sub>Fe<sub>2</sub>), is the material with the highest known magnetostriction at room temperature; it changes size when subjected to a magnetic field. It was initially developed for sonar detectors, but is now used in actuators, magnetomechanical sensors and transducers for acoustics or ultrasound.



*A magnetostrictive actuator  
(Image courtesy Wikipedia)*

### Typical uses

Sonar; acoustic and ultrasound transducers; actuators; magnetomechanical sensors; diesel injectors

### General properties

|         |      |                   |
|---------|------|-------------------|
| Density | 9250 | kg/m <sup>3</sup> |
|---------|------|-------------------|

### Thermal properties

|                          |             |            |
|--------------------------|-------------|------------|
| Melting point            | 962 - 1540  | °C         |
| Maximum service temp.    | 129 - 176   | °C         |
| Thermal conductivity     | 10.9 - 13.2 | W/m.°C     |
| Thermal expansion coeff. | 12.2 - 14.9 | µstrain/°C |

### Mechanical properties

|                      |           |     |
|----------------------|-----------|-----|
| Young's modulus      | 30 - 80   | GPa |
| Shear modulus        | 17.6 - 20 | GPa |
| Bulk modulus         | 34 - 47   | GPa |
| Poisson's ratio      | 0.3       |     |
| Yield strength       | 28 - 40   | MPa |
| Tensile strength     | 28 - 40   | MPa |
| Compressive strength | 305 - 880 | MPa |
| Hardness - Vickers   | 120 - 221 | HV  |

### Functional Properties

|                        |      |
|------------------------|------|
| Ferromagnetic          | True |
| Giant magnetostriction | True |

### Magnetic properties

|                                     |             |         |
|-------------------------------------|-------------|---------|
| Curie temperature (magnetic)        | 677 - 680   | °C      |
| Coercive force H <sub>c</sub>       | 5430 - 6570 | A/m     |
| Saturation induction B <sub>s</sub> | 0.91 - 1.1  | T       |
| Max permeability                    | 9 - 12      |         |
| Saturation magnetostriction         | 1400 - 2000 | µstrain |

### Electrical properties

|                        |         |         |
|------------------------|---------|---------|
| Electrical resistivity | 58 - 63 | µohm.cm |
|------------------------|---------|---------|

## 3.3 Magnetocaloric Materials

**Magnetocaloric effect.** When a magnetic material is subject to a magnetic field, its magnetic moments tend to align with the applied field. This leads to an increase in the order in the material and so a decrease in entropy. The entropy change occurs extremely quickly, so under adiabatic condition this is compensated by an increase in lattice entropy leading to a corresponding increase in temperature. Removing the magnetic field adiabatically allows disordering of the magnetic moments, increasing the magnetic entropy, decreasing its lattice entropy and causing a temperature decrease.

**Magnetic entropy change.** One measure of the magnetocaloric effect is the size of the isothermal entropy change caused by a magnetic field when the change in magnetization occurs infinitely slowly. This must be calculated indirectly either from isothermal M(H) curves using the Maxwell formula:

$$\Delta S_m = \int_0^{H_{max}} \left( \frac{\partial M}{\partial T} \right)_H dH$$

or from measurements of the heat capacity:

$$\Delta S_m = \int_0^{T^*} \frac{\Delta C_p(T)}{T} dT$$

where  $\Delta C_p(T)$  is the change in heat capacity of the materials when the field is applied.

**Adiabatic temperature change.** When a field  $M$  is applied to magnetocaloric materials the temperature change is instantaneous and thus adiabatic. Unlike the entropy change, the adiabatic temperature change of a material can be directly measured. The size of the temperature change  $\Delta T_{ad}$  when a field  $B$  is applied is given by.

$$\Delta T_{ad} = - \int_0^{B^*} \frac{T}{\Delta C_p(T, B)} \left( \frac{\partial M}{\partial T} \right)_B dB$$

where  $\Delta C_p(T, B)$  is the heat capacity at temperature  $T$  and magnetic induction is  $B$ .

**Applications.** The maximum temperature change per unit applied field generated by the magnetocaloric effect is typically of the order of 2K per tesla. This on its own is not large, but when combined with a heat pump it is large enough to change the temperature by 50K. Magnetic refrigerators are about 30% more efficient than conventional vapor-compression refrigerators and are more reliable because they have fewer moving parts. They do not require the ecologically harmful coolants used in conventional refrigerators. With new legislation restricting the emission of greenhouse gases, both the improvement in efficiency and reduction in harmful coolants mean that magnetic refrigerators may displace conventional refrigeration in everything from domestic fridge-freezers to industrial air conditioning. They are already commercially available.

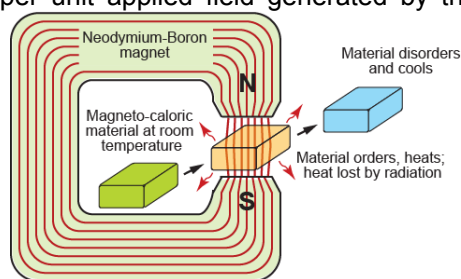


Figure 3.11. Magnetocaloric cooling.

### Performance metrics and charts for magnetic refrigeration.

**Adiabatic temperature change.** Commercial devices require a large adiabatic temperature change (Gschneider and Pecharsky, 2008). The temperature change increases with the magnetic field, but fields above 1.6T are impractical for domestic applications.

**Operating and Transition/Curie temperature.** The best magnetocaloric materials combine several contributions to the total entropy variation; the giant magneto-caloric effect (MCE) of  $\text{Gd}_5(\text{Si}_{1-x}\text{Ge}_x)_4$ , for example, results from the coupling between a first-order structural transition lattice and the magnetic transition. The MCE of FeRh arises from the coupling between electronic and magnetic transitions. The peak magnetocaloric response comes at the magnetic transition temperature (usually the Curie temperature) because it is here that the magnetization changes most rapidly with temperature and  $\partial M / \partial T$  is greatest. Useful magneto-caloric materials thus have a Curie temperature. The Curie temperature can be tuned by slight compositional changes to maximize efficiency for a particular application (Bruck, 2005).

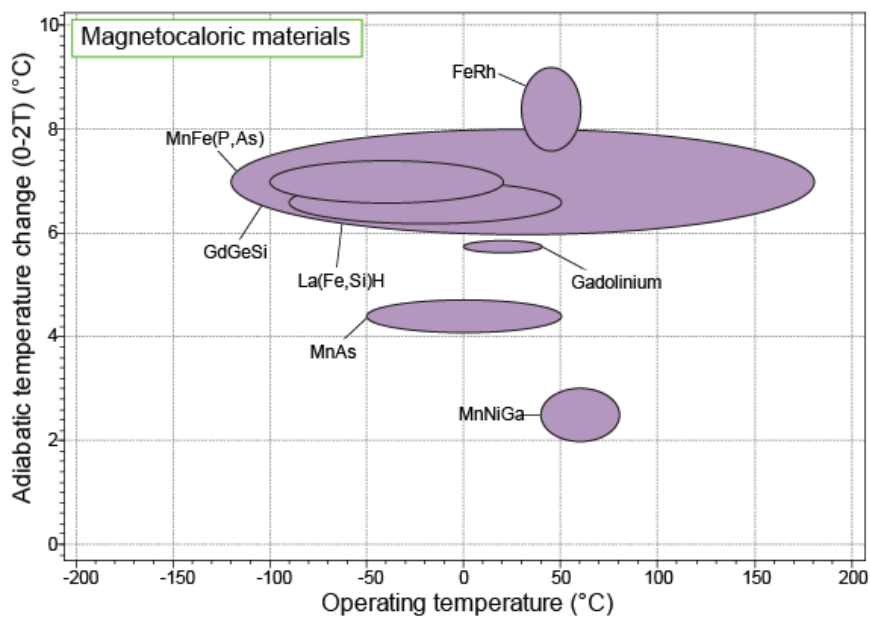


Figure 3.12. The operating temperature range and adiabatic temperature change of commonly researched magnetocaloric systems

Figure 3.12 shows how common materials fit these metrics. At present gadolinium is the most commonly used magnetostrictive material but there is much interest in the newer alloy systems, particularly those not containing rare-earth elements, which are expensive and can be difficult to source.

The content of a typical record is shown below. Further information for magnetostrictive materials can be found in Thshin and Spichkin (2003), Gschneider and Pecharsky (2008), Bruck (2005) and Olabi and Grunwald (2008).

*Typical record for a magnetocaloric material*

## **Gadolinium**

### **The material**

Gadolinium, Gd, is a ferromagnetic rare-earth metal most notable for its strong magnetocaloric effect. Until recently, it was used mostly as an addition to iron-chromium alloys to increase their workability and high temperature resistance. However, due to its Curie temperature being close to room temperature and it demonstrating a strong magnetocaloric effect, there has been much recent work looking at using gadolinium for magnetic refrigeration.



*Gadolinium. (Image courtesy Wikipedia Commons)*

### **Typical uses**

Stainless steel addition; MRI contrast agent; phosphors for color TV tubes; refractories; magnetic refrigeration

### **General properties**

|         |             |                   |
|---------|-------------|-------------------|
| Density | 7850 - 7950 | kg/m <sup>3</sup> |
| Price   | 124 - 206   | USD/kg            |

### **Thermal properties**

|                         |           |            |
|-------------------------|-----------|------------|
| Melting point           | 1300      | °C         |
| Maximum service temp    | 40        | °C         |
| Minimum service temp    | 0         | °C         |
| Thermal conductivity    | 10 - 10.5 | W/m.°C     |
| Specific heat capacity  | 225 - 240 | J/kg.°C    |
| Thermal expansion coeff | 6 - 9     | μstrain/°C |

### **Mechanical properties**

|                      |           |                      |
|----------------------|-----------|----------------------|
| Young's modulus      | 54 - 57   | GPa                  |
| Shear modulus        | 20 - 24   | GPa                  |
| Bulk modulus         | 36 - 40   | GPa                  |
| Poisson's ratio      | 0.26      |                      |
| Yield strength       | 160 - 300 | MPa                  |
| Tensile strength     | 170 - 430 | MPa                  |
| Compressive strength | 160 - 300 | MPa                  |
| Elongation           | 4 - 9     | % strain             |
| Hardness - Vickers   | 50 - 105  | HV                   |
| Fracture toughness   | 45 - 90   | MPa.m <sup>0.5</sup> |

### **Functional Properties**

|                |      |
|----------------|------|
| Ferromagnetic  | True |
| Magnetocaloric | True |

### **Magnetic properties**

|                              |    |    |
|------------------------------|----|----|
| Curie temperature (magnetic) | 20 | °C |
|------------------------------|----|----|

### **Magnetocaloric properties**

|                              |                   |
|------------------------------|-------------------|
| Tunable transition temp      | False             |
| Operating temperature        | 0 - 40 °C         |
| Mag. entropy change (0-2T)   | 4.5 - 5.5 J/kg.°C |
| Adiabatic temp change (0-2T) | 5.7 - 5.8 °C      |

### **Electrical properties**

|                        |           |         |
|------------------------|-----------|---------|
| Electrical resistivity | 132 - 150 | μohm.cm |
|------------------------|-----------|---------|

## 4. Semiconductors

### Overview. Materials and Functional Attributes

| Record name         |                    |
|---------------------|--------------------|
| Aluminum antimonide | Aluminum arsenide  |
| Aluminum phosphide  | Antimony telluride |
| Bismuth telluride   | Cadmium selenide   |
| Cadmium sulfide     | Cadmium telluride  |
| Cobalt antimonide   | Gallium arsenide   |
| Gallium antimonide  | Gallium phosphide  |
| Gallium nitride     | Indium antimonide  |
| Germanium           | Indium antimonide  |
| Indium arsenide     | Indium phosphide   |
| Lead telluride      | Silicon            |
| Manganese silicide  | Silicon germanium  |
| Silicon carbide     | Zinc selenide      |
| TAGS                | Zinc telluride     |
| Zinc sulfide        |                    |

| Attribute                       | Unit                 |
|---------------------------------|----------------------|
| Band-gap                        | eV                   |
| Electron mobility               | cm <sup>2</sup> /V.s |
| Hole mobility                   | cm <sup>2</sup> /V.s |
| Intrinsic carrier concentration | cm <sup>-3</sup>     |
| Saturated drift velocity        | cm/s                 |
| Seebeck coefficient             | μV/°C                |
| zT max                          | -                    |
| Temperature at zT max           | °C                   |
| zT (temperature dependent)      | -                    |

### 4.1 Semiconductors

**Semiconductors.** Electrons in solids occupy discrete energy level that are grouped into bands (Figure 4.1). The electrical properties of a material are dependent on the properties of the lowest unoccupied energy levels, known as the **conduction band** and the highest occupied energy levels, known as the **valence band**. In good electrical conductors, there is overlap between the valence and conduction bands, allowing electrons to pass from the one to

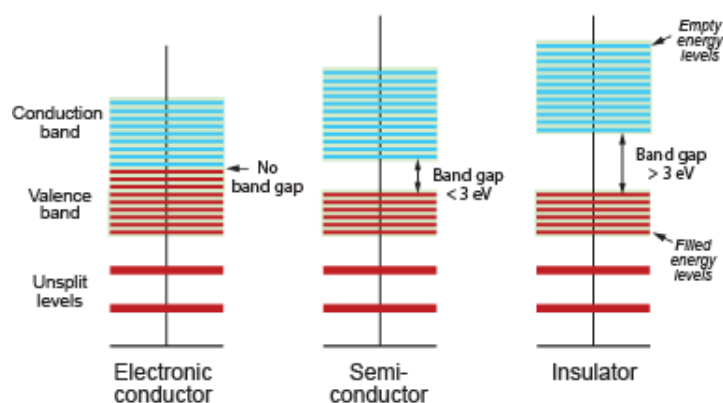


Figure 4.1: Flat band diagrams of different classes of material

the other and move easily through the material. In insulators there is a large **band-gap** (of order 3.5 to 6 eV) separating the full valence band and the empty conduction band, which means that electrons remain localized in the valence band and are not free to move.

The distinguishing features of semiconductors as compared to metals and insulators are:

- Semiconductors have a band-gap of order 1 eV.
- Semiconductors can be subdivided into two classes: intrinsic (pure) and extrinsic (doped).
- Doping with selected impurities allows wide control of electrical conductivity by changing the concentrations of the two carrier-types: electrons and holes.
- Electrical conductivity depends on temperature, illumination and electric field.
- Semiconductors can emit visible radiations.

**Semiconducting materials (Figure 4.2).** Inorganic semiconductors belong to the group IV elements or compounds (eg. SiC), compounds of groups III and V (eg. GaN), and those of groups II and VI (eg. CdSe). In addition, some more complex inorganic compounds (eg. Bi<sub>2</sub>Te<sub>3</sub>) can exhibit semiconducting behavior and have unique properties such as thermoelectric behavior that will be described in the next section.

|    |    |    |     |    |    |    |     |
|----|----|----|-----|----|----|----|-----|
|    |    |    | III | IV | V  | VI | VII |
|    |    |    | B   | C  | N  | O  | F   |
|    |    |    | Al  | Si | P  | S  | Cl  |
| I  | II |    |     |    |    |    |     |
| Cu | Zn | Ga | Ge  | As | Se | Br |     |
| Ag | Cd | In | Sn  | Sb | Te | I  |     |
| Au | Hg | Tl | Pb  | Bi | Po | At |     |

III-V  
 II-VI

Figure 4.2: Materials displaying semiconducting properties. They are isoelectronic of group IV in which the valence band is full.

**Intrinsic (pure) semiconductors** have an energy gap between the valence and conduction band but this is small enough that electrons can be thermally excited across it, allowing limited conduction. At 0K semiconductors are electrically insulating. As the temperature is raised, increasing numbers of electrons are thermally activated (“promoted”) into the conduction band leaving a positively charged region (a “hole”) in the valence band. Collective movement of the valence electrons can cause this hole to move through the valence band. Thus conduction in semiconductors involves two types of charge carrier – electrons and holes – and increases with temperature.

The density of charge carriers in a semiconductor ( $n$  for electrons,  $p$  for holes) is dependent on the ease of thermal excitation of electrons across the band-gap. For an *intrinsic* semiconductor, the number of conduction electrons,  $n$ , and of holes,  $p$ , are equal:

$$n = p = N_o \exp\left(\frac{-E_g}{2kT}\right)$$

where  $N_o$  is a constant,  $k$  is the Boltzmann constant and  $E_g$  is the band-gap energy.

The band-gap depends on the bond length, increasing as the atomic radius decreases. For this reason the conductivity changes from electrical insulator to semiconductor to metallic conductor in the sequence C (diamond) to Si to Ge to Sn in the group IV elements (Table 4.1).

Table 4.1 Lattice parameter and band-gap of group IV elements

| Element     | Bond length, Å | Band-gap (eV) |
|-------------|----------------|---------------|
| C (diamond) | 3.6            | 5.5           |
| Silicon     | 5.43           | 1.1           |
| Germanium   | 5.65           | 0.67          |
| Tin         | 6.5            | 0             |

**Extrinsic semiconductors** acquire their properties through doping. The concentrations of promotable electrons and holes now differ and depend on the nature and concentration of the dopant. Doping silicon with a group V element, which has 5 valence electrons, provides four electrons to the covalent bonding and leaves one electron loosely bound to the dopant-atom.

This fifth electron is referred as a donor electron because the energy required to elevate it into the conduction band is less than that for the electrons involved in the covalent bonding (Fig. 4.3a). Since the donor atoms provide electrons to the conduction band without creating holes in the valence band, there are more electron charge carriers than holes, and the doped material is referred as an n-type semiconductor (n for negatively charged). Similarly, it is possible to create an excess of holes by doping Si with group III atoms (Fig. 4.3b). Materials doped in this way are known as p-type semiconductors.

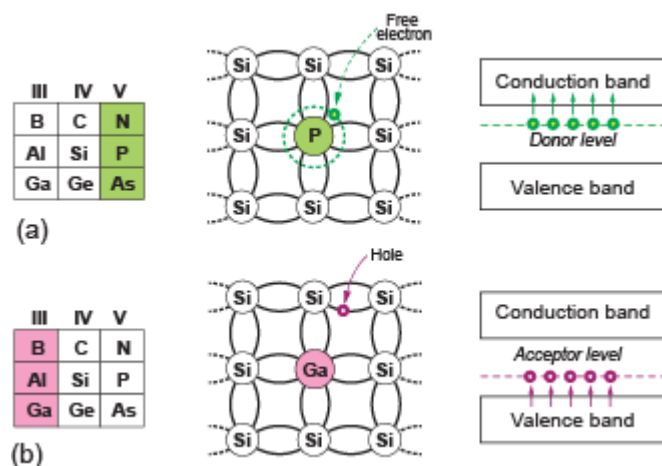


Figure 4.3. n and p-type doping

**Degeneracy.** When the concentration of doping elements is small the donated electrons or holes do not interact and the dopant energy level remains discrete (non-degenerate). As the dopant concentration increases donor electrons or holes start to interact, splitting the single discrete donor energy into a wider band that may overlap the bottom of the conduction band in n-doped material or the top of the valence band in p-doped material. This type of semiconductors is called degenerate.

**Mobility.** Electron movement is easier in semiconductors than metals because the conduction band in semiconductors is virtually empty, giving the charge carriers high **mobility**. At low drift velocities the velocity  $v$  of a charge carrier in a field  $E$  is proportional to the electric field:

$$v = \mu E$$

where  $\mu$  is the mobility. Thus the conductivity  $\sigma$  of an intrinsic semiconductor is given by

$$\sigma = ne(\mu_e + \mu_h)$$

where  $\mu_e$  is the electron mobility,  $\mu_h$  that of the holes,  $n$  is the charge carrier density and  $e$  is the charge on one electron. At high fields the carrier velocity is no longer proportional to the field but reaches a maximum, the **saturation drift velocity** because charge carriers interact with the lattice leading to loss of energy through the generation of phonons or photons.

**Band-gap type.** In real semiconductors, the band structure is more complex than the flat-band model that Figure 4.1 suggests. The energy of the valence and conduction bands varies depending on the momentum of the charge carriers as in Figure 4.4. In *direct semiconductors*, the minimum energy of the conduction band occurs at the same momentum as the maximum energy of the valence band. In *indirect* semiconductors the maxima and minima do not coincide. This means that for an electron to be promoted to the conduction band, a phonon must also be created to conserve momentum.

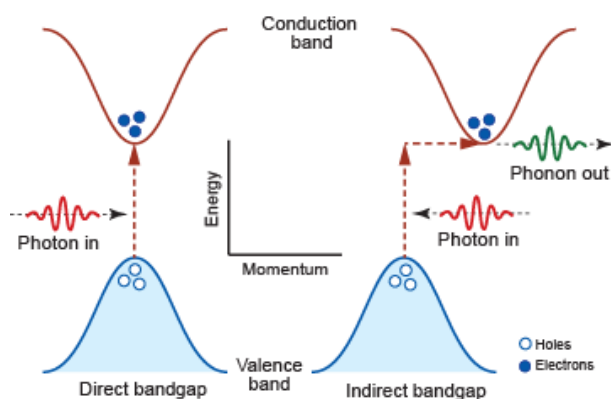


Figure 4.4: Promotion of an electron in direct and indirect semiconductors

### Applications.

**The transistor.** A semiconductor transistor consists of n- and p-type materials joined at a junction. Current flows through the device only when a voltage is applied to a third junction.

**Optical devices.** A light emitting diode (LED) is also based on a p-n junction. When a voltage is applied, electrons are driven from the n-type to the p-type and the reverse for holes. At the boundary between the two regions, holes and electrons combine (i.e. conduction band electrons are de-excited back to the valence band). Conservation of energy requires the emission of a photon of frequency proportional to the energy gap.

$$E_g = h\nu$$

LEDs emit light of only one frequency, green or redder frequencies if the band-gap is narrow, blue or UV when it is wide. White light is created by using a wide band-gap LED to stimulate emission of the light from a phosphor coating. Efficient LEDs require direct semiconduction. This is because the de-excitation of a valence electron in an indirect semiconductor annihilates phonons to conserve momentum, dissipating energy and reducing efficiency.

**Photovoltaics.** If photons of high enough energy are incident on a p-n junction, they excite electrons into the valence band, creating holes at the same time. The electrons are swept clear of the junction, leading to an excess of electrons in the n-type region, of holes in the p-type region and a potential difference across the cell from which power can be drawn. Conventional solar cells, based on single-crystal silicon, are relatively efficient and reliable but are expensive because the silicon must be very pure. Cells base on thin films of amorphous silicon or cadmium telluride have lower collection efficiency but can be made by vapor deposition, use less material, and are cheaper than single-crystal silicon.

### Performance metrics and charts for semiconductors.

**Transistors and power electronics** are devices designed to amplify and/or switch an electrical signal. The switching speed of a semiconductor is characterized by the Keyes figure of merit, KM (Chow and Tyagi, 1994):

$$KM = \lambda \left( \frac{v_s}{\epsilon_R} \right)^{1/2}$$

where  $v_s$  is the saturation drift velocity,  $\epsilon_R$  is the dielectric constant and  $\lambda$  is the thermal conductivity. It appears as a diagonal lines on the chart of Figure 4.5. Silicon ranks well by this

index and, additionally, is relatively easily processed to the high purities required to grow single crystals by the Czochralski technique. Processing gallium phosphate or gallium nitride in this way is more difficult.

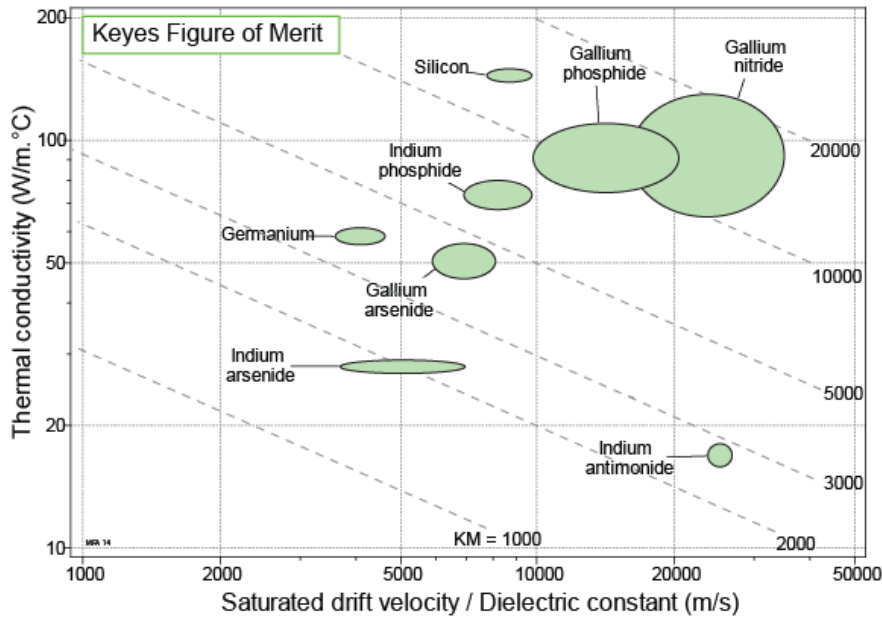


Figure 4.5. The Keyes figure of merit for the switching speeds of semiconductors. The lines of gradient -0.5 represent materials with equal figure of merit.

The Baliga index BHF<sub>M</sub> is a figure of merit for high power and high frequency devices.

$$BHF_M = \mu E_c^2$$

where  $\mu$  is the charge carrier mobility and  $E_c$  is the dielectric breakdown potential. It is shown as the diagonal contours on Figure 4.6. Gallium arsenide, indium phosphide and gallium nitride have high values of this index. They are used in radio frequency, high power electronics such as in mobile communication.

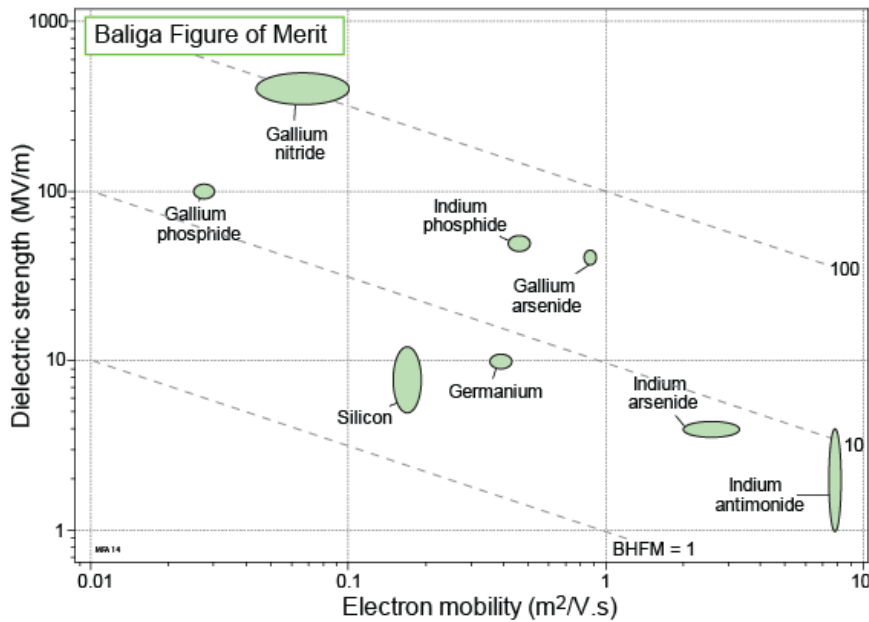


Figure 4.6. The Baliga high frequency figure of merit for high frequency and power transistors. The lines of gradient -0.5 show equal figure of merit

*Light emitting devices.* The wavelength  $\lambda_l$  of radiation emitted when an electron falls from the conduction band to the valence band depends directly on the band-gap energy  $E_g$  :

$$\lambda_l = \frac{hc}{E_g}$$

where  $c$  is the velocity of light.

For elemental semiconductors, the band-gap decreases as the bond strength decreases and the lattice constant increases; the progression C → Si → Ge is an example. The III-V and II-VI semiconductors, show a similar trend (Figure 4.7). While there is no simple expression relating the band-gap and the lattice parameter,  $a_o$ , empirically,  $E_g$  is approximately proportional to  $1/a_o^2$  for the group-IV elemental semiconductors. For the same lattice constant, the band-gap increases with increasing ionicity, as in the sequence IV–IV → III–V → II–VI. The best example is the sequence Ge → GaAs → ZnSe all of which have almost the same lattice constant.

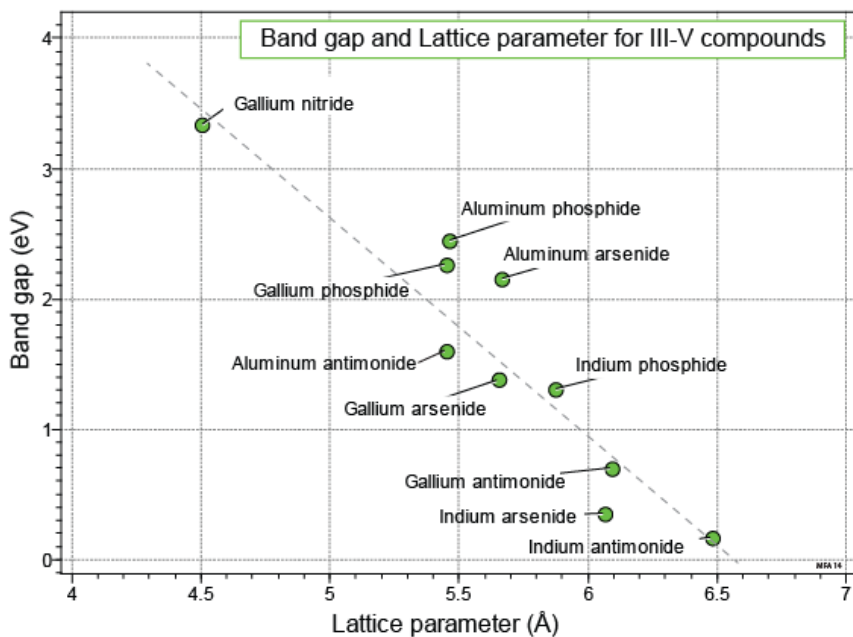


Figure 4.7. The band-gap energy of semiconductors plotted as a function of lattice constant of the crystal structure for III-V semiconductors.

Figure 4.8 is a chart of the emission wavelength and the band-gap energy, with optical wavelengths shown as colors<sup>1</sup>. Dopants such as nitrogen and zinc allow the band-gap to be adjusted, as does alloying similar semiconductors such as the combinations  $GaAs_xP_{1-x}$  and  $Ga_xIn_{1-x}P$ . Silicon, germanium and gallium phosphide are indirect semiconductors and so are not as efficient at light emission, but gallium phosphide is still commonly used because it has a convenient emission wavelength.

<sup>1</sup> Planck's constant  $h = 6.6 \times 10^{-34}$  J/s; speed of light  $c = 3 \times 10^8$  m/s; 1 eV =  $1.6 \times 10^{-19}$  J; thus  $\lambda_l$  (in microns) =  $1.23/E_g$  ( $E_g$  in eV)

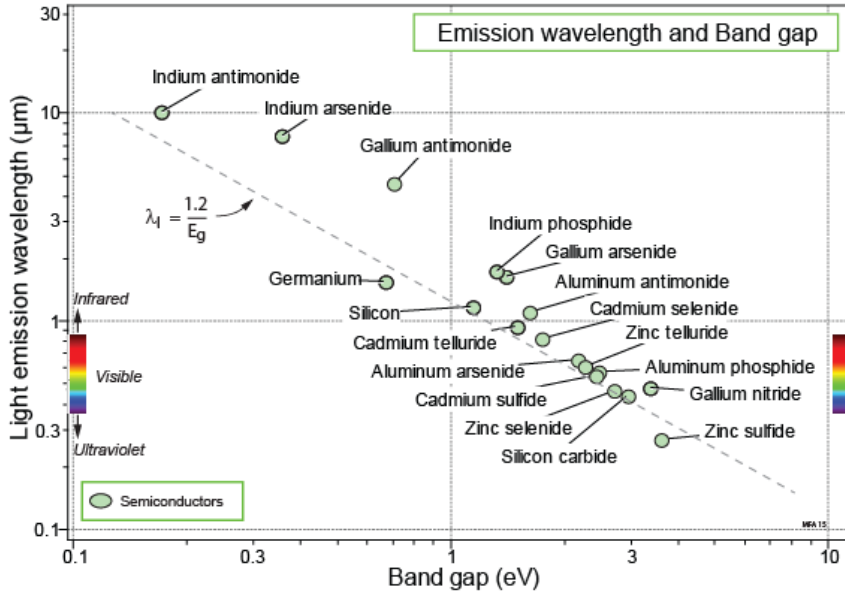


Figure 4.8. The emission wavelength of semiconductors plotted as a function of the band-gap energy. Si, Ge and GaP are indirect semiconductors, making them less efficient emitters of light, although GaP is still commonly used

Figure 4.9 shows the correlation between the charge carrier concentration and the energy band-gap.

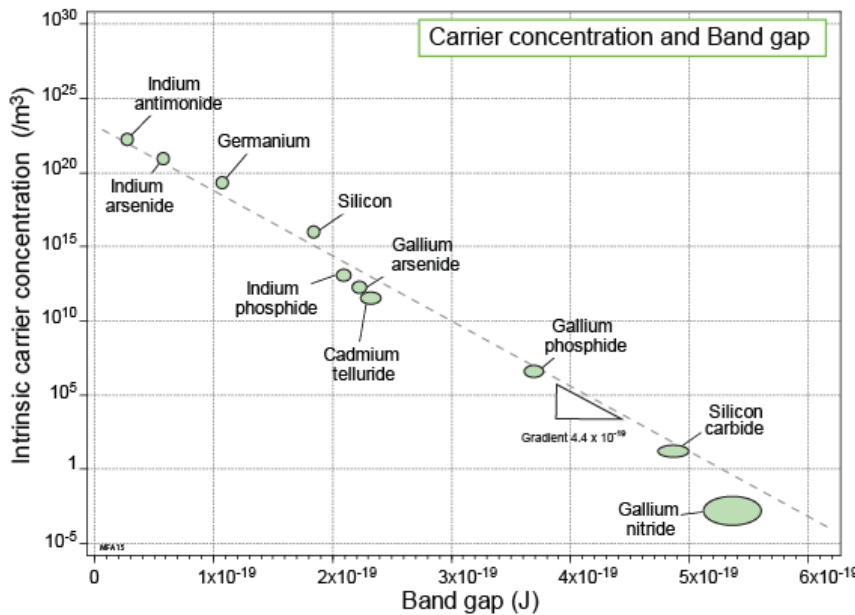


Figure 4.9. The intrinsic carrier concentration and band-gap of semiconductors in SI units. The line of gradient  $-4.4 \times 10^{-19}$  shows the expected relationship at 300K

**Photovoltaic solar cells.** Photovoltaics require a band-gap energy that is a little less than the average photon energy in sunlight (about 1.5 eV). The most commonly used material is silicon ( $E_g = 1.15\text{eV}$ ) (Cardarelli, 2000) but its indirect band-gap means that silicon solar cells are less efficient than materials with a direct band-gap. Thin film solar cells based on direct semiconductors such as cadmium telluride ( $E_g = 1.44\text{-}1.5\text{eV}$ ), have higher efficiency than alternatives like polysilicon.

As mentioned earlier, the intrinsic carrier concentration is given by.

$$n = p = N_o \exp\left(\frac{-E_g}{2kT}\right)$$

Figure 4.9 is a chart of  $\log(n)$  and  $E_g$ . The data, in SI units, should lie on a line of slope  $-2kT$  where  $k$  is the Boltzmann constant and  $T$  is the absolute temperature. For a temperature of 300K this gives a gradient of  $-4.4 \times 10^{-19}$  decades per Joule, well matched on the figure.

The electron mobility  $\mu$  depends on on its charge,  $e$ , its life-time  $\tau$  and its effective mass  $m^*$

$$\mu = \frac{e\tau}{m^*}$$

An electron moving through a crystal behaves as if it had an effective mass  $m^*$  that differs from that of an electron in free space because the lattice field influences its motion. The effective mass takes into account the particle mass both of these:

$$m^* = m_o \frac{E_g}{2E_o}$$

where  $m_o$  and  $E_o$  are the mass and energy of the free electron. Thus:

$$\mu = \frac{2e\tau E_o}{m_o} \frac{1}{E_g}$$

Figure 4.10 compares this predicted relationship between  $\mu$  and  $E_g$  with data for the semiconductors contained in the database.

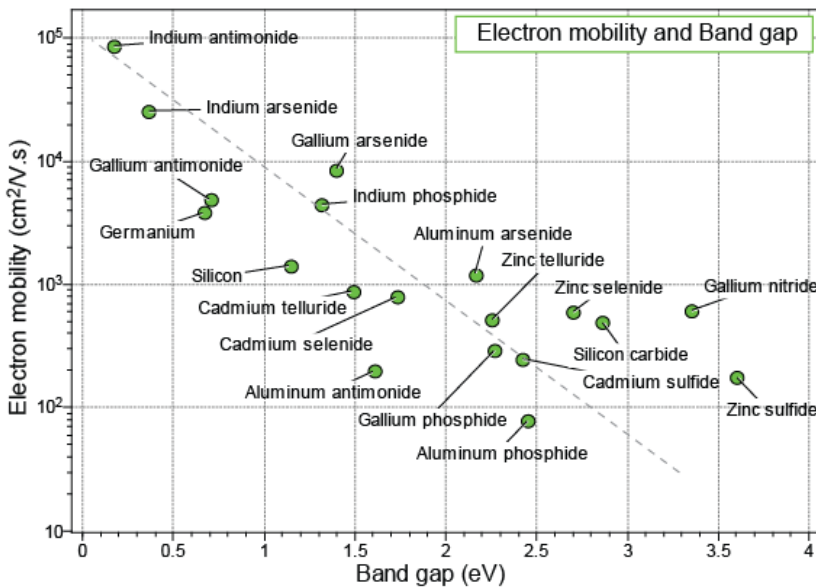


Figure 4.10. The electron mobility and band-gap of semiconductors showing the exponential decrease in mobility with increasing band-gap

The content of a typical record is shown below. Further information for semiconductors can be found in Cardarelli (2000), and Chung (2010).

*Typical record for a semiconducting material*

## Gallium arsenide

### The material

Gallium arsenide, GaAs, is a III-V type semiconductor with a direct band-gap. It has much better electronic properties than silicon at high frequency and so is often seen in high electron mobility transistors for frequencies >600GHz. The direct band-gap of GaAs means it is an efficient absorber and emitter of light, meaning it is commonly used for infra-red LEDs and laser diodes in the near-visible region.



*Gallium arsenide single crystal (Image courtesy of Biotain Crystal Co.)*

### Typical uses

Radio frequency transistors; IR Laser diodes and LEDs; mobile phones; radar systems

### General properties

|                   |      |                   |
|-------------------|------|-------------------|
| Lattice parameter | 5.65 | Å                 |
| Density           | 5320 | kg/m <sup>3</sup> |

### Thermal properties

|                         |           |            |
|-------------------------|-----------|------------|
| Melting point           | 1240      | °C         |
| Thermal conductivity    | 46 - 56   | W/m.°C     |
| Specific heat capacity  | 330 - 350 | J/kg.°C    |
| Thermal expansion coeff | 5.4 - 5.7 | µstrain/°C |

### Mechanical properties

|                    |              |                      |
|--------------------|--------------|----------------------|
| Young's modulus    | 82.7 - 85.9  | GPa                  |
| Shear modulus      | 32.9 - 42.77 | GPa                  |
| Bulk modulus       | 75.3 - 97.9  | GPa                  |
| Poisson's ratio    | 0.31         |                      |
| Hardness - Vickers | 500 - 690    | HV                   |
| Fracture toughness | 0.44 - 0.51  | MPa.m <sup>0.5</sup> |

### Optical properties

|                  |           |
|------------------|-----------|
| Refractive index | 3.3 - 3.8 |
|------------------|-----------|

### Functional Properties

|               |      |
|---------------|------|
| Semiconductor | True |
|---------------|------|

### Electrical properties

|                        |                       |
|------------------------|-----------------------|
| Semiconductor          |                       |
| Electrical resistivity | 1e10 - 3.3e14 µohm.cm |
| Dielectric constant    | 10.4 - 13.2           |
| Dielectric strength    | 37.3 - 45.1 MV/m      |

### Semiconductor properties

|                          |                                  |
|--------------------------|----------------------------------|
| Group type               | III-V                            |
| Band-gap                 | 1.35 - 1.43 eV                   |
| Band-gap type            | Direct                           |
| Electron mobility        | 8500 - 8800 cm <sup>2</sup> /V.s |
| Hole mobility            | 400 - 450 cm <sup>2</sup> /V.s   |
| Intrinsic carrier conc.  | 1800 - 2100 /mm <sup>3</sup>     |
| Saturated drift velocity | 7.2e4 - 9e4 m/s                  |
| Emission wavelength      | 1.64 - 1.66 µm                   |

## 4.2 Thermoelectric Materials

The applications of thermoelectricity, such as thermocouples, thermoelectric coolers, and thermoelectric generators, involve energy conversion from heat to electrical energy or the reverse, and rely on three fundamental thermoelectric phenomena: the Seebeck, the Peltier and the Thompson effects.

### Thermoelectric effects.

*The Seebeck effect*, discovered in 1821, describes the appearance of an electrical potential when two materials are joined together and placed in a thermal gradient. In a thermoelectric material free electrons or holes transport both charge and heat. To a first approximation, the electrons and holes in a thermoelectric semiconductor behave like a gas of charged particles. If a normal (uncharged) gas is placed in a box within a temperature gradient the gas molecules at the hot end move faster than those at the cold one. The faster hot molecules diffuse further than the cold ones, leading to a net build-up of molecules at the cold end as in Figure 4.11. The density gradient

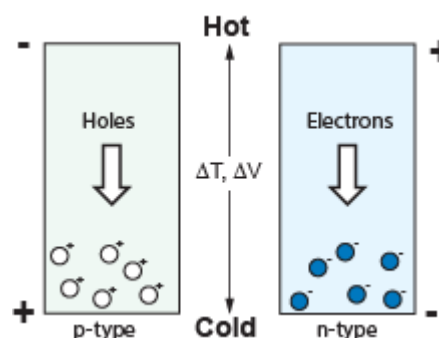


*Figure 4.11: The Seebeck effect – charge carriers diffuse from hot to cold*

drives the molecules to diffuse back towards the hot end so that, at steady-state, the two effects exactly compensate and there is no net flow.

Electrons and holes behave in a similar way. Because they carry charge, the temperature gradient creates a charge gradient between the hot and cold ends of the material; the charge gradient tends to push the charges back to the hot end. If the free charges are positive (the material is p-type), positive charge builds up at the cold face, which acquires a positive potential. If instead they are negative (n-type material) the cold face acquires a negative potential.

The Seebeck coefficient  $S$  ( $\mu\text{V}/^\circ\text{C}$ ) is a measure of the change in voltage  $\Delta V$  induced across a thermoelectric material by a thermal gradient  $\Delta T$ . For small temperature changes, the Seebeck coefficient is given by.

$$S = - \frac{\Delta V}{\Delta T}$$

A positive Seebeck coefficient indicates that the charge carriers are positive (holes); a negative Seebeck coefficient means that they are electrons. (To allow comparison of both p-type and n-type thermoelectrics, only the absolute value of the Seebeck coefficient is recorded in the database.) The density and mobility of charge carriers changes with temperature; for this and other reasons the Seebeck coefficient depends strongly on temperature.

*The Peltier (inverse thermoelectric) effect* was discovered by Jean-Charles Peltier in 1834. When a current is passed across a junction of two materials, heat is absorbed or rejected at the junction depending on the direction of the current. The rate  $dQ/dt$  at which the heat is either deposited or removed is

$$\frac{dQ}{dt} = \Pi i$$

where  $\Pi$  is the Peltier coefficient and  $i$  is the current.

*The Thomson effect links* the Seebeck and the Peltier effects. It describes the generation or absorption of heat when a material is held in a temperature gradient while carrying an electrical current. Thomson showed that the Peltier coefficient is related to the Seebeck coefficient by.

$$\Pi = TS$$

where  $T$  is the temperature of the thermoelectric material.

**Applications.** A thermoelectric device consists of an array of thermoelectric couples consisting of n-type and p-type semiconductor legs connected electrically in series through metallic contact pads and thermally in parallel. There are two types – thermoelectric generators (TEGs) and thermoelectric refrigerators (Figure 4.12). Until now, thermoelectric devices are used in niche applications where price (aerospace) or quality (small appliances such as camping products) are immaterial.

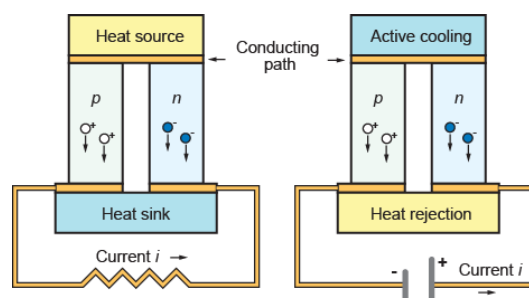


Figure 4.12: Thermoelectric generation (left) and refrigeration (right).

**Thermoelectric refrigeration.** When a voltage is applied across the thermoelectric, the Peltier effect causes one junction to cool. The efficiency of conversion from electrical to thermal energy is about one quarter that of conventional refrigeration techniques, but Peltier coolers are compact, they have no moving parts and a long life. Feedback circuitry allows for precise temperature control (to within 0.01°C), attractive for use in laser applications.

**Thermoelectric generation.** When placed in a thermal gradient, thermoelectric materials generate a voltage through the Seebeck effect. For current to flow, it is necessary to have both a p-type and an n-type thermoelectric so that charge can be conserved. Thermoelectrics allow electrical power to be harvested from waste heat such as that of car exhaust systems. Their other main use is in spacecraft. When far from the sun, solar cells become ineffective. The alternative is a radioisotope thermoelectric generator (RTG) that uses the decay of a radioactive isotope to generate a thermal gradient. PbTe/TAGS and SiGe unicouples have been used on more than 60 planetary rovers and space probes.

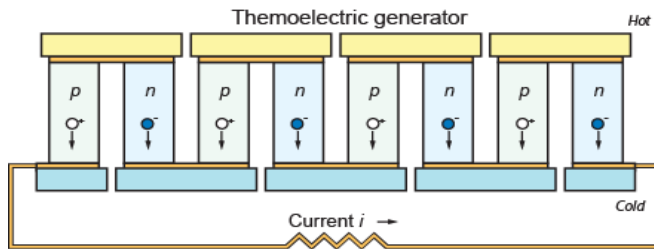


Figure 4.13: Schematic multicouple TE generator

The power output ( $P$ ) and conversion efficiency ( $\eta$ ) of TEGs depend on intrinsic material properties and device architecture. Referring to Figure 4.13, the power output is

$$P \propto NAS^2\kappa_e\Delta T^2, \text{ and}$$

$$\eta \propto \eta_c \frac{\sqrt{1+zT} - 1}{\sqrt{1+zT} + T_c/T_h}$$

where  $N$  is the number of thermocouples in the device (Fig. 4.13),  $A$  the cross-section area of thermoelements,  $\Delta T$  the temperature difference between the hot ( $T_h$ ) and cold sides ( $T_c$ ),  $S$  the Seebeck coefficient,  $\kappa_e$  the electrical conductivity,  $\eta_c$  is the Carnot efficiency and  $zT$  is the figure of merit.

**Figure of merit  $zT$ , power factor ( $PF = S^2\kappa_e$ ) and material choice.** To provide power a thermoelectric material must have a high electrical conductivity  $\kappa_e$  to allow easy movement of charge carriers and reduce resistive losses, and a high Seebeck coefficient  $S$  to generate a voltage. This combination is captured by the power factor (PF)

$$PF = \kappa_e S^2$$

In addition a low thermal conductivity is required to maintain a steep temperature gradient between the hot and cold side, which is reflected into the figure of merit,  $zT$  :

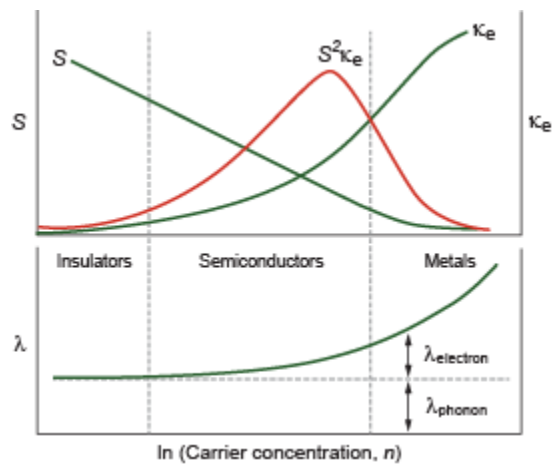


Figure 4.14: The dependence of the power factor (numerator of  $z$ ) and the properties that make it up on carrier concentration.

$$zT = \frac{\kappa_e S^2}{\lambda} T$$

where  $T$  is temperature and  $\lambda$  is the thermal conductivity. Thus good materials for thermoelectric applications combine a large Seebeck coefficient with high electrical conductivity and low thermal conductivity – a combination not easily achieved. The Seebeck coefficient and the electrical conductivity are both functions of the free charge carrier concentration (Figure 4.14) in such a way that the power factor  $\kappa_e S^2$ , has a maximum at carrier concentration around  $10^{26} \text{ m}^{-3}$ .

Heat is transported through materials by moving charge carriers (electron conductivity  $\lambda_e$ ) and by lattice vibrations (phonon conductivity  $\lambda_l$ ). The total thermal conductivity is

$$\lambda_{total} = \lambda_e + \lambda_l$$

In metals, electron transport dominates and the same electrons provide electrical conductivity with the result that  $\lambda_e$  is directly proportional to  $\kappa_e$  (the Wiedemann-Franz law):

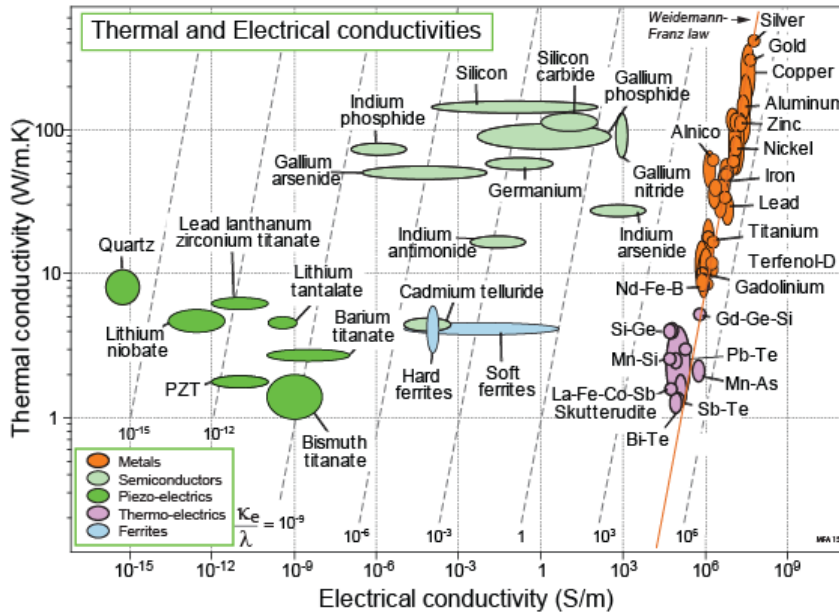
$$\lambda_e = \kappa_e L T$$

where  $L = 2.44 \times 10^{-8} \text{ watt.ohm/K}^2$  is the Lorentz number and  $T$  the temperature. Thus the lattice thermal conductivity is the only independent term entering  $zT$ . According to the Debye model,  $\lambda_l$  is given by

$$\lambda_l = C_v v_s \Delta_{ph}$$

where  $C_v$  is the lattice specific heat,  $v_s$  the speed of sound and  $\Delta_{ph}$  the phonon mean free path. The lattice thermal conductivity is reduced by scattering phonons. In a perfect lattice there is little scattering,  $\Delta_{ph}$  is large and  $\lambda_l$  is high. By contrast, in amorphous structures (glasses)  $\Delta_{ph}$  approaches the inter-atomic distance. Glasses have the lowest lattice thermal conductivities but also very low electrical conductivities, making them unsuitable as thermoelectrics. The ideal is summed up in the concept of the “phonon-glass/electron-crystal”, a thermoelectric material with the electrical properties of a crystalline material and the thermal properties of an amorphous material. This state is approached by scattering phonons in different frequency ranges using alloying (mass fluctuation scattering), crystal lattice engineering with rattler atoms in structural cages, and microstructure engineering accomplished by precipitation scattering and interface scattering.

**Performance metrics and charts for thermoelectric materials.** A good thermoelectric material requires both a high electrical conductivity and a low thermal conductivity. Figure 4.15 shows these two properties for common materials. Metals lie along a straight line of slope 1 (the Wiedemann-Franz law, already mentioned). The other possibility for increasing thermopower is to increase the Seebeck coefficient, but this conflicts with the requirement for high electrical conductivity because a high Seebeck coefficient requires a low carrier concentration (Tritt and Subramanian, 2006). Figure 4.16 shows that good thermoelectric materials are those that combine a high Seebeck coefficient.  $S$  with a high conductivity ratio



$$\kappa_e / \lambda.$$

Figure 4.15. Thermal and electrical conductivity. Good thermoelectric materials (in purple) need low thermal and high electrical conductivity, the bottom right corner of the plot. The line of slope 1 marks the Wiedemann-Franz law.

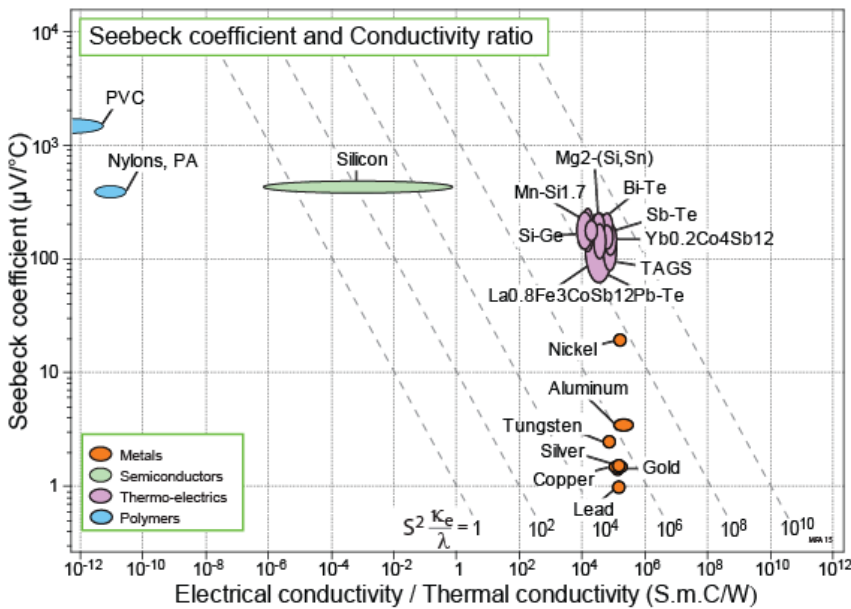


Figure 4.16. Seebeck coefficient and conductivity ratio for thermoelectric materials. A few standard engineering materials are also included. The dashed lines (gradient 0.5) represent contours of equal thermoelectric figure of merit

Further insight into thermoelectric-property space is given by Figure 4.17, on which the components of the merit index  $zT$  - the power factor and the thermal conductivity - are plotted. The best thermoelectric materials lie in the top left corner.

**Temperature dependence.** The thermal and electrical conductivities and the Seebeck coefficient of semiconductors all depend on temperature (Figure 4.18). This is reflected in the

temperature dependence of the index  $zT$ . The database allows the value of  $zT$  to be selected at a user-defined temperature. The thermoelectric performance of lead telluride, shown in the Figure 4.18, is poor at room temperature but good at 350°C, making it suitable for use in high temperature thermoelectric generators such as the radioisotope thermoelectric generators used in exploratory satellites and planetary rovers.

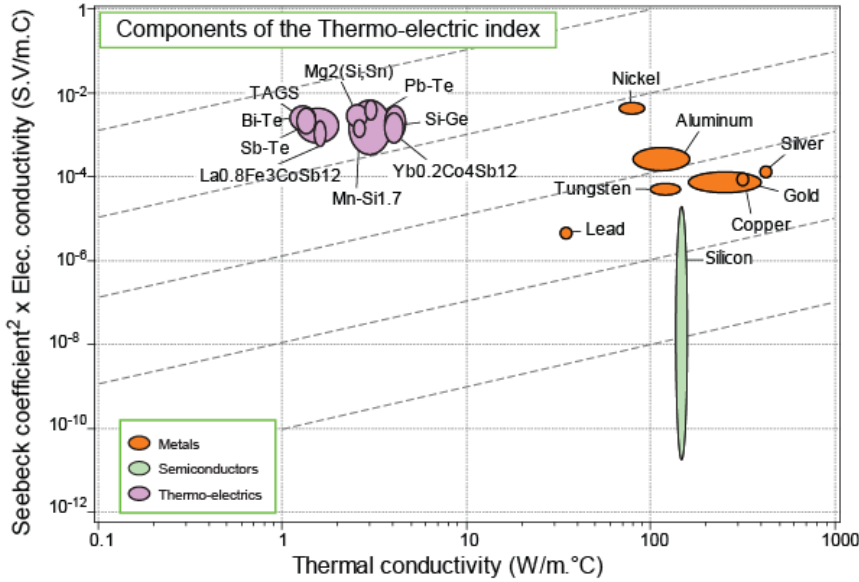


Figure 4.17. The components of the figure of merit  $zT$

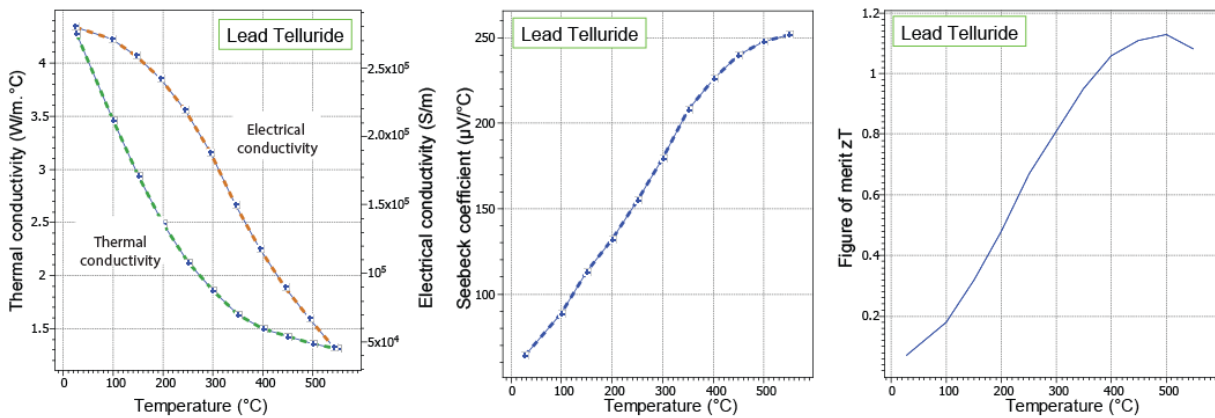


Figure 4.18. The Seebeck coefficient, electrical resistivity and thermal conductivities of  $PbTe$  as a function of temperature.

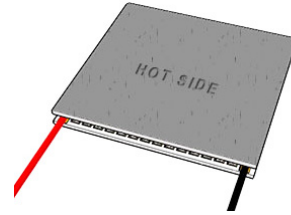
The content of a typical record is shown below. Further information for thermoelectric materials can be found in Tritt and Subramanian (2006), and Snyder and Toberer (2008).

*Typical record for a thermoelectric material*

**Bismuth telluride**

**The material**

Bismuth telluride, Bi<sub>2</sub>Te<sub>3</sub>, is a semiconductor that demonstrates strong thermoelectric properties when combined with antimony or selenium. It has a high thermoelectric figure of merit near room temperature, making it particularly useful for portable refrigerators and for controlling the temperature of microchips or lasers. It is also commonly used for energy generation near to ambient temperatures, but its low melting point precludes it from use in higher temperature applications.



A Bismuth telluride thermoelectric unit (Image courtesy of Custom Thermoelectric)

**Typical uses**

Portable refrigerators; thermal energy harvesting near ambient temperature; microchip cooling; temperature control in lasers

**General properties**

Density 7860 kg/m<sup>3</sup>

**Thermal properties**

Melting point 585 °C  
 Maximum service temp. 297 - 360 °C  
 Thermal conductivity 1.3 - 1.5 W/m.°C  
 Thermal expansion coeff. 14.4 - 21.3 μstrain/°C

**Mechanical properties**

Young's modulus 45 - 55 GPa  
 Shear modulus 18 - 22 GPa  
 Bulk modulus 29 - 35 GPa  
 Poisson's ratio 0.24  
 Yield strength 20 - 40 MPa  
 Tensile strength 20 - 40 MPa

**Functional Properties**

Semiconductor True  
 Thermoelectric True

**Electrical properties**

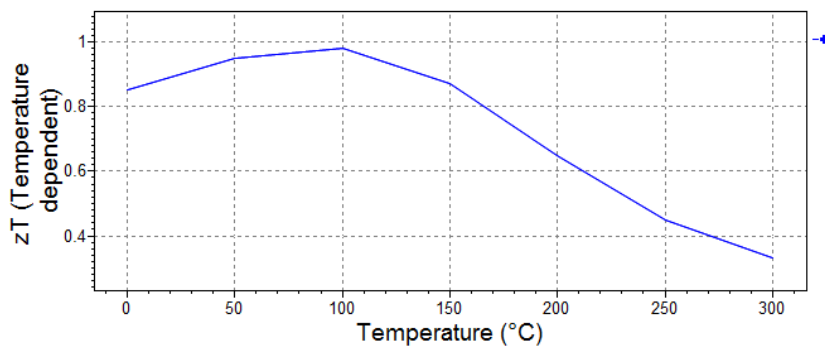
Semiconductor  
 Electrical resistivity 600 - 2000 μohm.cm

**Semiconductor properties**

Band-gap 0.16 - 0.21 eV  
 Band-gap type Indirect  
 Electron mobility 1140 cm<sup>2</sup>/V.s  
 Hole mobility 680 cm<sup>2</sup>/V.s

**Thermoelectric properties**

Seebeck coefficient 140 - 250 μV/°C  
 zT max 0.9 - 1.1  
 Temperature at zT max 70 - 110 °C  
 zT (T-dependent) 0.9  
 Parameters: Temperature = 25°C



## 5. Case Studies

### 5.1: Electric energy storage

The energy density of a capacitor with a single dielectric layer (Figure 5.1) increases with the square of the field  $E$  :

$$\text{Energy density} = \frac{1}{2} \epsilon_r \epsilon_o E^2$$

where  $\epsilon_r$  is the relative permittivity (dielectric constant) and  $\epsilon_o$  the permittivity of vacuum ( $8.854 \times 10^{-12}$  F/m). An upper limit for  $E$  is the dielectric strength,  $E_b$ , setting an upper limit for energy density:

$$\text{Maximum energy density} = \frac{1}{2} \epsilon_r \epsilon_o E_b^2$$

This upper limit is plotted in Figure 5.2, which illustrates the enormous gains that ferroelectric ceramics offer. PZT has the highest value (and it is used for high performance capacitors) but barium titanate is the more usual selection because it is cheaper, easier to process, and lead-free.

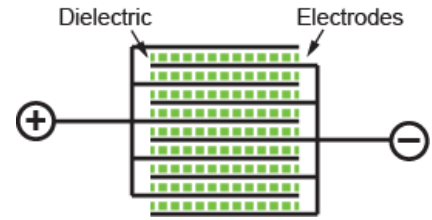


Figure 5.1 A capacitor stores electrical energy

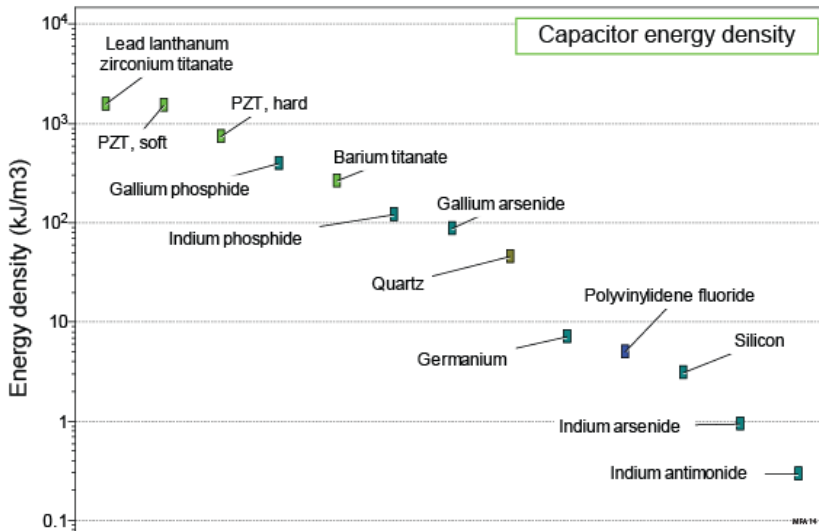


Figure 5.2. A plot showing the maximum energy density made possible by dielectric materials. The ferroelectric ceramics have the highest values.

## 5.2: Accelerometers and kinetic energy harvesting

**Accelerometers.** Piezo-electric accelerometers rely on the inertia of a mass  $m$  to generate a force

$$F = ma$$

when subjected to an acceleration or a deceleration  $a$ . If this force is applied to the end of a beam to which a thin layer of piezoelectric material is bonded, the piezoelectric layer is stretched or compressed (Figure 5.3). The resulting charge that appears on the piezoelectric can be detected and, if necessary, used to trigger a response if the acceleration or deceleration exceeds a critical value. For this, and piezoelectric material with a high piezoelectric charge coefficient  $d_{33}$  is desirable. Figure 5.4a is a plot of this coefficient. Soft lead zirconium titanate (PZT) has the highest value of this coefficient. If the additional constraint that the piezoelectric must not contain toxic materials is applied, the top three materials in Figure 5.4a are eliminated, leaving barium titanate as the best choice.

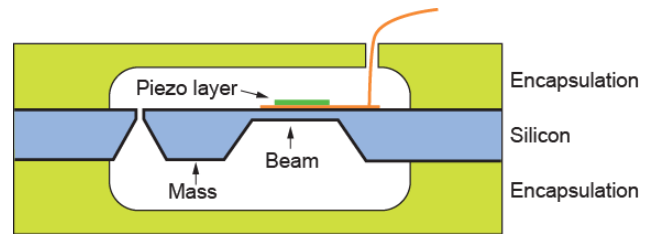


Figure 5.3. One configuration for a simple piezoelectric accelerometer or energy-harvesting device.

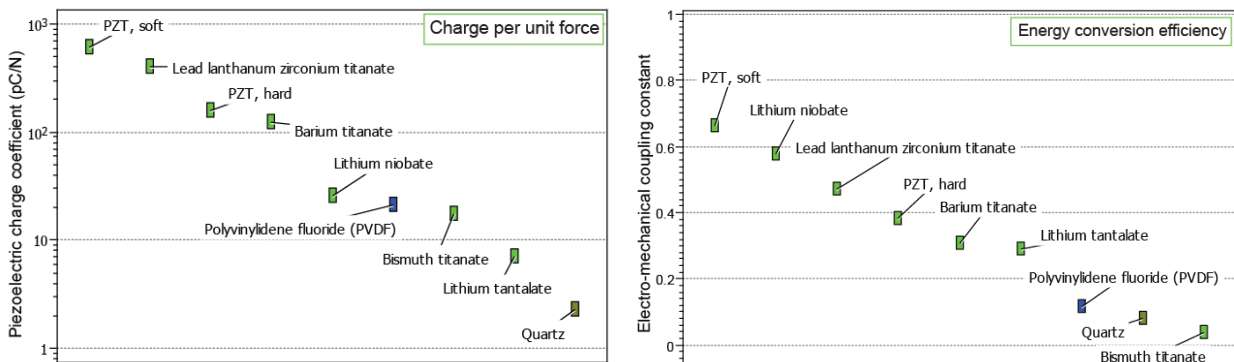


Figure 5.4(a) The piezoelectric charge coefficient and (b) the electro-mechanical coupling constant.

**Energy harvesting.** Small portable electronic devices operate with low electrical drain, but their batteries require regular charging. Mechanical energy from vibration or cyclic movement is present almost everywhere. The configuration shown in Figure 5.3 allows electrical power to be harvested from acceleration and deceleration associated with mechanical vibration. Here the conversion efficiency of mechanical to electrical energy is the dominant consideration. Figure 5.4b shows the electro-mechanical coupling constant, which is a measure of this efficiency. Once again, soft PZT is the best choice. If toxic materials are eliminated, lithium niobate emerges as the optimum choice. In this application the configuration of the device plays a more important role: ideally, the mass and beam should be chosen such that the resonant frequency of the system lies at or near the frequency of vibration from which the energy is drawn.

“Vibration energy harvesting with aluminum nitride-based piezoelectric devices” R Elfrink, T M Kamel, M Goedbloed, S Matova, D Hohlfeld, Y van Andel and R van Schaijk, J. MICROMECH. MICROENG. Vol. 19 (2009)

### 5.3: Energy harvesting from waste heat

To provide power a thermoelectric material must have a high Seebeck coefficient  $S$  to generate a voltage, a high electrical conductivity  $\kappa_e$  to reduce resistive losses and a low thermal conductivity  $\lambda$  to maintain a steep temperature gradient between the hot and cold side of the generator. This combination is captured by the figure of merit,  $zT$  :

$$zT = \frac{S^2 \kappa_e}{\lambda} T$$

where  $T$  is mean temperature at which the device operates. Thus good materials for thermoelectric applications combine a large Seebeck coefficient with high electrical conductivity and low thermal conductivity – a combination not easily achieved. All the material properties in this expression for  $zT$  depend on temperature, so the best choice of material depends on the temperature of the heat source.

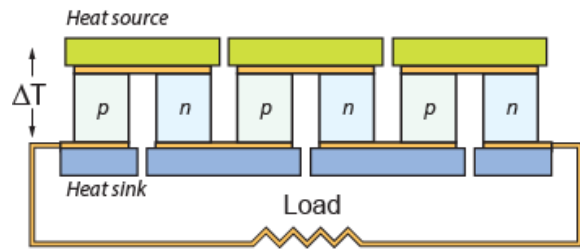


Figure 5.5. Schematic multicouple thermoelectric generator

**Energy harvesting from automobile exhaust.** At least a third of the energy used by a car is lost as waste heat. Some of this can be converted back to useful electrical energy using thermoelectric generators. Figure 5.6(a) shows the material property combination

$$z = \frac{S^2 \kappa_e}{\lambda}$$

evaluated at 250 C – an assumed temperature for the exhaust manifold. The best choices of material are TAGS (an alloy of tellurium, antimony, germanium and silver) and cobalt arsenide Skutterudite,  $\text{Yb}_{0.2}\text{Co}_4\text{Sb}_{12}$ .

**Energy harvesting from domestic waste hot water.** A lot of heat goes out with the bath water. Materials for harvesting electrical energy from a source at 50 C (a hot bath) are shown in Figure 5.6(b). In this application the best choices are antimony telluride or bismuth telluride.

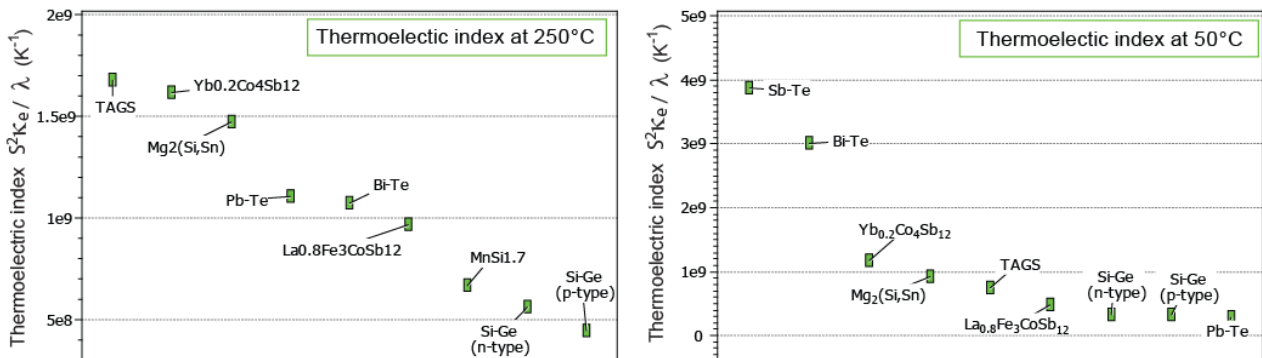


Figure 5.6(a) The thermoelectric index evaluated at 250 C; (b) the same index evaluated at 50C.

## 6. Conclusions

The CES EduPack Functional Materials database extends the standard Level 2 database by the inclusion of 43 new records and 40 new attributes. They describe the properties of piezo, pyro and ferroelectrics materials, magnetic, magnetostrictive and magnetocaloric materials, and semiconducting and thermoelectric material. Science notes and example plots illustrate the content and application of the new database. The extended database becomes a powerful resource to support the teaching of Materials Science.

## Acknowledgements

We wish to acknowledge the important support of our colleagues at Granta Design, Cambridge, the Cambridge University Engineering Department, the Department of Materials Science, Cambridge and the Bordeaux INP & Institut de Chimie de la Matière Condensée de Bordeaux.

## Bibliography

- Baliga, B.J.** *Power semiconductor device figure of merit for high-frequency applications.* Electron Device Letters, IEEE, (1989), pp. 455-457.
- Beeby, S. P., Tudor, M. J. and White, N. M.** *Energy harvesting vibration sources for microsystems applications.*, Meas. Sci. Technol., (2006) Vol. 17, pp. 175-195.
- Beerman, H. P.,** *Investigation of pyroelectric material characteristics for improved infrared detector performance.* s.l. : Pergamon Press (1975), Infrared Physics, Vol. 15, pp. 225-231.
- Biswas, K., He, J., Blum, I.D., Wu, C-I., Hogan, T.P., Seidman D.N., Dravid, V.P. and Kanatzidis, M.G.** *High-performance bulk thermoelectrics with all-scale hierarchical architectures* Nature, (2012) Vol. 489 pp. 414 - 418
- Bowen, C. R. and Topolov, V. Yu.** *Piezoelectric sensitivity of PbTiO<sub>3</sub>-based ceramic/polymer composites with 0-3 and 3-3 connectivity.* Acta Materialia, (2003) Vol. 51, pp. 4965-4976.
- Bruck, E.,** *Developments in Magnetocaloric Refrigeration.* J. Phys. D: Appl. Phys., (2005) Vol. 38, pp. 381-391.
- Cardarelli, F.,** *Materials Handbook: A Concise Desktop Reference.* s.l. : Springer, (2000).
- Chow, T. P. and Tyagi, R.,** *Wide Bandgap Compound Semiconductors for Superior High-Voltage Unipolar Power Devices.* 8, s.l. : IEEE, Transactions on Electron Devices, (1994) Vol. 41, pp. 1481-1483.
- Chung, Deborah D.L.** *Functional Materials: Electrical, Dielectric, Electromagnetic, Optical and Magnetic Applications.* s.l. : World Scientific, (2010).
- Colin, M., Basrour, S., Rufer, L., Bantignies, C. and Nguyen-Dinh, A.** *Highly Efficient Low-Frequency Energy Harvester using Bulk Piezoelectric Ceramics.* Journal of Physics Conference Series, (2013) Vol. 476.
- Ertuğ, B.** *The Overview of the Electrical Properties of Barium Titanate.* 8, (2013), AJER, Vol. 2, pp. 1-7.
- Gschneider, K. A. and Pecharsky, V. K.** *Thirty years of near room temperature magnetic cooling: Where we are today and future prospects.*, International Journal of Refrigeration, (2008) Vol. 31, pp. 945-961.
- Haertling, G. H.** *Ferroelectric Ceramics: History and Technology.* 4, (1999), J. Am. Ceram. Soc., Vol. 82, pp. 797-818.
- Holterman, J. and Groen, P.** "An introduction to piezoelectric materials and applications", Applied Piezo (2013). ISBN. 978-90-819361-1-8
- Holterman, J. and Groen, P.** *An introduction to piezoelectric materials and applications,* Applied Piezo (2013). ISBN. 978-90-819361-1-8

**Jaffe, B. Jaffe, H. and Cook W.R.** "Piezoelectric Ceramics" Academic Press (1971) ISBN-13. 978-0124332614

**Jaffe, B. Jaffe, H. and Cook W.R.** *Piezoelectric Ceramics*, Academic Press (1971) ISBN-13. 978-0124332614

**Liu, J.H., Jiang, C.B. and Xu, H.B.** *Giant Magnetostrictive Materials.*, Sci. China Tech. Sci., (2012) Vol. 55, pp. 1319-1326.

**Moulson A.J and Herbert J.M.** "Electroceramics. Materials, Properties, Applications" 2<sup>nd</sup> edition, Wiley-Blackwell (2010). ISBN-13. 978-0471497486

**Olabi, A-G. and Grunwald, A.,** *Design and Application of Magnetostrictive Materials.* Materials & Design, (2008), Vol. 29, pp. 469-483.

**Olabi, A-G., and Grunwald, A.** *Design and Application of Magnetostrictive Materials.* Materials & Design, (2008) Vol. 29, pp. 469-483.

**Pei, Y., Shi, X., LaLonde, A., Wang, H., Chen, L. and Snyder, G.J.** *Convergence of electronic bands for high performance bulk thermoelectrics.* Pei, Y, et al., et al., Nature, (2011) Vol. 473, pp. 66-69.

**Snyder, G. J. and Toberer, E. S.** *Complex thermoelectric materials.*, Nature Materials, (2008) pp. 105-114.

**Tishin, A. M. and Spichkin, Y. I.** *The Magnetocaloric Effect and its Applications.* s.l. . IOP Publishing Ltd, (2003).

**Tritt, T. M. and Subramanian, M.A.** *Thermoelectric Materials, Phenomena and Applications: A Bird's Eye View.*, MRS Bulletin, (2006) Vol. 31, pp. 188-194.

**Uchino, K.** *Ferroelectric Devices.* s.l. : Marcel Dekker, Inc., (2000).

Ueno, T., Miura, H. and Yamada, S. *Evaluation of a miniature magnetostrictive actuator using Galfenol under tensile stress.* J. Phys. D: Appl. Phys., (2011) Vol. 44.

**Yang, J. and Caillat, T.** *Thermoelectric Materials for Space and Automotive Power Generation.* MRS Bulletin, (2006) Vol. 31, pp. 224-229.



**GRANTA**  
TEACHING RESOURCES

Granta's Teaching Resources website aims to support teaching of materials-related courses in Engineering, Science and Design.

The resources come in various formats and are aimed at different levels of student.

The website also contains other resources contributed by faculty at the 1000+ universities and colleges worldwide using Granta's CES EduPack.

The teaching resource website contains both resources that require the use of CES EduPack and those that don't.